In this study, we attempted to develop p-BLs that have the potential to be useful contrast agents and efficient delivery tools for gene therapy. We examined the therapeutic effect of gene delivery using the hindlimb ischemia mouse model.

2. Materials and methods

2.1. Preparation of liposomes and BLs

To prepare liposomes for BLs that do not contain cationic lipid, 1,2-dipalmitoyl-sn-glycero-phosphatidylcholine (DPPC) and 1,2-distearoylphosphatidylethanolamine-methoxy-polyethylene glycol (PEG_{2000}) were mixed at a molar ratio of 94:6. Both lipids were purchased from NOF Corporation (Tokyo, Japan). For BLs containing cationic lipid, 1,2-stearoyl-3-trimethylammonium-propane (DSTAP), 1,2-distearoyl-3-dimethylammonium-propane (DSDAP), and dimethyldioctadecylammonium bromide (DDAB) from Avanti Polar Lipids (Alabaster, AL) were used. Liposomes with various lipid compositions were prepared using the reverse phase evaporation method as described previously [19]. Briefly, DPPC, cationic lipid, and PEG_{2000} were mixed at a molar ratio of 64:30:6 and dissolved in 1:1 (*v*/*v*) chloroform/diisopropylether. HEPES-buffered saline (HBS: 150 mM NaCl, 10 mM HEPES, pH 7.0) was added to the lipid solution, and the mixture was sonicated and then evaporated. The organic solvent was completely removed, and the size of the liposomes was adjusted to less than 200 nm using extruding equipment and a sizing filter (Nuclepore Track-Etch Membrane, 200 nm pore size; Whatman plc, UK). After sizing, the liposomes were filter-sterilized using a 0.45-μm syringe filter (Asahi Techno Glass Co., Chiba, Japan).

The liposome concentration was determined using a phosphorus assay. BLs were prepared from liposomes and perfluoropropane gas (Takachiho Chemical Inc. Co. Ltd., Tokyo, Japan). First, 5-mL sterilized vials containing 2 mL of liposome suspension (lipid concentration: 1 mg/mL) were filled with perfluoropropane gas, capped, and then pressurized with 7.5 mL of perfluoropropane gas. The vials were placed in a bath sonicator (42 kHz, 100 W, Bransonic 2510J-DTH; Branson Ultrasonics Co., Danbury, CT) for 5 min to form BLs. The zeta potential and mean size of the BLs were determined using a light scattering method with a zeta potential/particle sizer, (Nicomp 380ZLS, Santa Barbara, CA). For preparation of BLs containing 1,2-dioleoyl-3-trimethylammonium-propane (DOTAP), we used phosphate-buffered saline (PBS) and 1,2-distearoyl-sn-glycero-3-phosphoethanolamine-N-[methoxy(polyethylene glycol)-750] (PEG_{750}) and DPPC, DOTAP, PEG_{2000}, and PEG_{750} were mixed at a molar ratio of 79:15:2:4, as described previously [21].

2.2. Ultrasound imaging

Male ICR mice were anesthetized, and injected with a BL solution in HBS into the tail vein. Examination of the heart or the ischemic hindlimb was performed using an Aplio80 ultrasound diagnostic machine (Toshiba Medical Systems, Tokyo, Japan) and a 12-MHz wideband transducer with contrast harmonic imaging at a mechanical index of 0.27. The mean intensity at various time points after injection into the ROI (region of interest) was quantified.

2.3. Cell lines and cultures

COS-7 cells were cultured in Dulbecco's modified Eagle's medium (DMEM; Kohjin Bio Co. Ltd., Tokyo, Japan), supplemented with 10% heat-inactivated fetal bovine serum (FBS; Equitech Bio Inc., Kerrville, TX), 100 units/mL penicillin, and 100 μg/mL streptomycin in a humidified atmosphere containing 5% CO_2 at 37 °C.

2.4. Plasmid DNA (pDNA)

The plasmid pcDNA3-Luc, derived from pGL3-basic (Promega, Madison, WI), is an expression vector encoding the firefly luciferase gene under the control of a cytomegalovirus promoter. The plasmid pBLAST-hbFGF (InvivoGen Inc., San Diego, CA) is an expression vector encoding the human bFGF gene controlled by an EF-1α promoter. The plasmid pBLAST is used as an empty vector control. Fluorescein-labeled pDNA (Label IT Plasmid Delivery Control) was purchased from Mirus (Madison, WI).

2.5. Preparation of p-BLs

For the preparation of p-BLs, adequate amounts of pDNA were added to BLs and gently mixed. To quantify the amount of pDNA loaded onto the BL surfaces, the BLs were centrifuged at 2000 rpm for 1 min, and the unbound pDNA was removed as previously reported [23]. The BL solution and aqueous solution containing unbound pDNA were then boiled for 5 min to solubilize the BLs and prevent background scattering. The optical density was measured at 260 nm using a spectrophotometer.

2.6. Stability of pDNA in the presence of serum

pDNA and p-BLs were incubated in 50% fetal bovine serum for 15–60 min. Serum was used without heat inactivation. To remove lipids and serum proteins, pDNA was extracted using a GenElute Mammalian Genome DNA Miniprep kit (Sigma–Aldrich, St. Louis, MO, USA). pDNA stability was confirmed via 1% agarose gel electrophoresis. The gel was stained with SYBR SAFE (Invitrogen Japan K.K., Tokyo, Japan) DNA stain and visualized under ultraviolet light.

2.7. Transfection of pDNA into cells using p-BLs and US

The day before transfection, 3×10^4 cells were seeded in the wells of a 48-well plate (Asahi Techno Glass Co., Chiba, Japan). p-BLs (BLs 60 μg, pcDNA3-Luc 5 μg) in culture medium containing 10% FBS were added to the cells. The cells were immediately exposed to US (Frequency, 2 MHz; duty, 50%; burst rate, 2.0 Hz; intensity 2.0 W/cm^2) for 10 s through a 6-mm diameter probe placed in the well. A Sonopore 3000 (NEPA GENE, Co., Ltd., Chiba, Japan) was used to generate the US. The cells were washed twice with culture medium and cultured for two days. To measure luciferase activity after transfection, cell lysate was prepared using a lysis buffer (0.1 M Tris–HCl (pH 7.8), 0.1% Triton X-100, and 2 mM EDTA). Luciferase activity was measured using a luciferase assay system (Promega, Madison, WI) and a luminometer (LB96V, Belthold Japan Co., Ltd., Tokyo, Japan). The activity is reported as relative light units (RLU) per mg of protein.

2.8. Hemolysis assay

Erythrocytes from mice were washed three times at 4 °C by centrifugation at 1000 rpm (Kubota 3700, Kubota, Tokyo, Japan) for 10 min and resuspended in PBS. A 5% stock suspension was prepared. Various BLs were added to the erythrocytes (BLs:stock suspension = 1:1) and incubated for 4 h at 37 °C. After incubation, the suspensions were centrifuged at 1000 rpm for 5 min, and supernatants were taken. Hemolysis was quantified by measuring the absorbance of hemoglobin at a wavelength of 540 nm. Lysis buffer was added to erythrocytes and used for the 100% hemolysis sample.

2.9. Hindlimb ischemia model

The ischemic hindlimb model was performed in five-week-old male ICR mice, as previously reported [24,25]. Briefly, animals were anesthetized, and a skin incision was made in the left hindlimb. After ligation of the proximal end of the femoral artery at the level of the inguinal ligament, the distal portion and all side branches were dissected and excised. The right hindlimb was kept intact to control the original blood flow. Measurements of the ischemic (left)/normal (right) limb blood flow ratio were performed for a set time using a laser Doppler blood flow meter (OMEGAFLO, FLO-C1).

2.10. In vivo luciferase gene delivery into the skeletal muscle of mice using BLs and US

Ten days after ligation of the femoral artery, a solution of 225 μL of p-BLs (BLs 200 μg, pcDNA3-Luc 50 μg) was injected into the tail vein, and the site of the hindlimb ischemia was immediately exposed to US (Frequency: 1 MHz, Duty: 50%, Burst rate: 2.0 Hz, Intensity: 1.0 W/cm^2, Time: 2 min). A Sonitron 2000 (NEPA GENE, Co., Ltd) was used as an ultrasound generator. Two days after transfection, the mice were euthanized. The thigh muscle in the US-exposed area was collected and homogenized in the lysis buffer. Luciferase activity was measured as described above.

2.11. The therapeutic effects of bFGF gene delivery with BLs and US

Ten and twelve days after ligation of the femoral artery, a solution of 225 μL of p-BLs (BLs 200 μg, pBLAST-hbFGF or pBLAST 50 μg) was injected into the tail vein, and US exposure (Frequency: 1 MHz, Duty: 50%, Burst rate: 2.0 Hz, Intensity: 1.0 W/cm^2, Time: 2 min) was immediately applied at the site of hindlimb ischemia. A Sonitron 2000 (NEPA GENE, Co., Ltd) was used as an ultrasound generator. Blood flow was measured several days after the second injection.

Four days after the second injection, the mice were euthanized, and the thigh muscle in the US-exposed area was collected. Total RNA was extracted with RNAiso Plus (Takara Bio Inc., Japan) according to the manufacturer's instructions. Complementary DNA was synthesized from 1 μg total RNA in a 20 μL reaction using Prime Script Reverse Transcriptase (Takara Bio Inc., Japan). Real-time RT-PCR was performed using an ABI PRISM 7000 Sequence Detection System instrument and software (Applied Biosystems Inc., Foster City, CA) with SYBR GreenER from Invitrogen. The primer sequences were previously described [21]. The amplification of the 18S ribosomal RNA gene was used as a control for RNA integrity and for assay normalization.

2.12. In vivo studies

Animal use and relevant experimental procedures were approved by the Tokyo University of Pharmacy and Life Sciences Committee on the Care and Use of Laboratory Animals. All experimental protocols for animal studies were in accordance with the Principle of Laboratory Animal Care in Tokyo University of Pharmacy and Life Sciences.

2.13. Statistical analyses

All data are represented as the mean ± SD (n = 3–6). Data were considered significant when $P < 0.05$. A t-test or one-way ANOVA was used to calculate statistical significance.

3. Results

We initially investigated the efficacy of BLs containing cationic lipids as US contrast agents. We performed US imaging of the heart after injecting of BLs via the tail vein and assessed the intensity of imaging effects. As shown in Fig. 1, all three types of BLs could be used as US contrast agents and are more stable than the BLs containing DOTAP that were previously reported [21,22]. BLs containing DSDAP were most effective of the three cationic lipids.

We examined the interaction of pDNA with each BL. As shown in Fig. 2, 30–40% of pDNA was loaded by BLs. The size of all BL types was 600–700 nm, and their zeta potential was almost neutral. Furthermore, adding pDNA to BLs did not result in a significant change in those physical properties (Table 1). We also investigated the stability of pDNA in 50% serum. Fig. 3 shows an image of free pDNA and p-BLs in the presence of serum for 15–60 min. The high-mobility band in the non-incubated samples was attributed to the most compact (supercoiled) form, whereas the other bands were considered to contain the non-supercoiled content in the plasmid preparation. The loss of the supercoil increased with longer incubation times; however, pDNA loaded onto BLs containing cationic lipid was more stable than free pDNA. Previously, we showed that p-BLs containing DOTAP could protect pDNA from serum components [21]. The result, however, showed a loss of the supercoiled conformation after incubation for 60 min, whereas the protective effects of the three types of BLs shown in this study could be observed even after incubation for 60 min.

To evaluate the ability of the BLs to induce cavitation which has been proposed as a driving force for gene transfection, we transfected pDNA into cells *in vitro*. Our results show that all BL types can be used for transfection and that BLs containing DSDAP were the most effective of the three cationic lipids (Fig. 4). We further investigated the cytotoxicity of type of BL. Cytotoxicity was absent after the transfection with p-BLs and US (data not shown). It has been reported that cationic liposomes often cause the agglutination

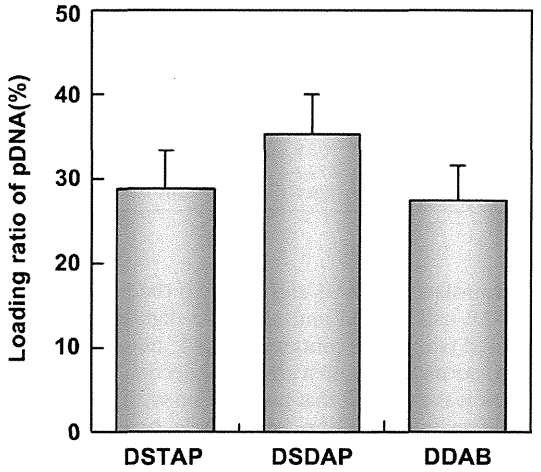

Fig. 2. Loading ratio of pDNA onto BLs. The ratio was calculated by measuring the optical density of a solution of p-BLs containing pDNA (15 μg) and various BLs (60 μg) after the removal of unbound pDNA via centrifugation.

of erythrocytes and high levels of hemolysis due to the interaction of the lipid component with the erythrocyte membrane [26,27]. Therefore, we also assessed the interaction of each BL with erythrocytes using an agglutination test and a hemolysis assay *in vitro*. No agglutination was observed in any BL type (data not shown). Furthermore, all BLs showed negligible hemolysis after a 4-hr incubation (Fig. 5). These results suggest that BLs containing cationic lipids have little effect on erythrocytes.

To evaluate the usability of p-BLs as a pDNA delivery tool via intravascular injection, we used the hindlimb ischemia mouse model. Before *in vivo* transfection using p-BLs and US, we first confirmed whether each p-BL was accessible to the ischemic hindlimb using US diagnostic equipment. The delivery of each p-BL to the ischemic hindlimb was observed and the signal intensity from p-BLs containing DSDAP had largest increase (Fig. 6a, b). We then transfected pDNA encoding the luciferase gene into the ischemic hindlimb. As shown in Fig. 6c, the combination of US and p-BLs containing DSDAP was the most effective. We also examined the

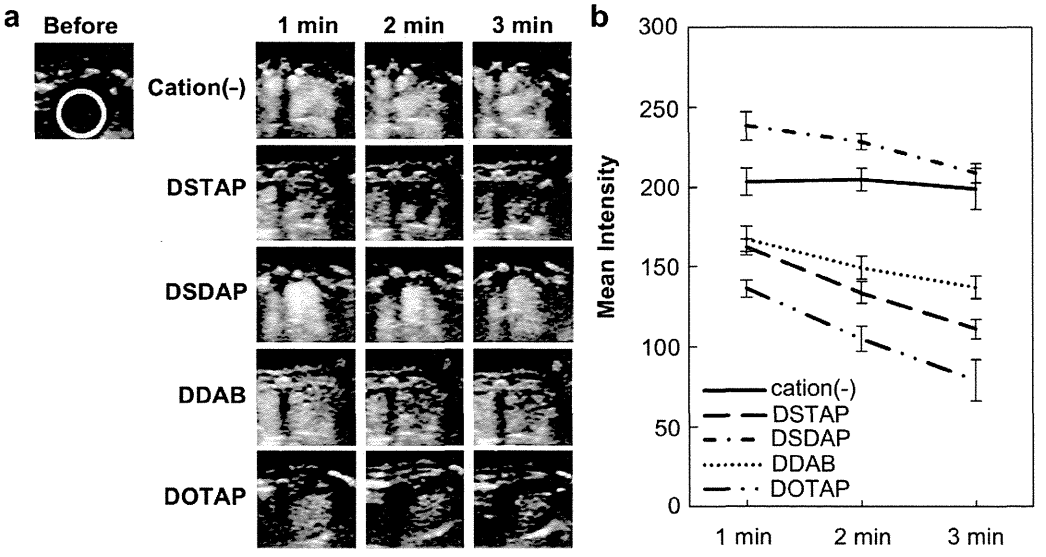

Fig. 1. (a) Ultrasonographic images of the heart using various BLs (1 mg/mL, 30 μL) containing cationic lipids 1–3 min after injection. Yellow circles show the region of interest (ROI). (b) Mean intensity of the pixels within the ROI. (For interpretation of the references to color in this figure legend, the reader is referred to the web version of this article.)

Table 1
Size and zeta potential of BLs or p-BLs.

	Mean size (nm)		Zeta potential (mV)	
	BLs	p-BLs	BLs	p-BLs
Cation(−)	636.5 ± 84.0	655.6 ± 72.2	0.22 ± 0.01	−0.39 ± 0.11
DSTAP	742.0 ± 85.6	906.9 ± 82.7	−0.36 ± 0.14	−1.81 ± 0.40
DSDAP	623.7 ± 82.8	577.2 ± 52.8	−0.17 ± 0.37	−2.66 ± 0.07
DDAB	700.8 ± 84.7	738.7 ± 97.5	−0.61 ± 0.85	−1.94 ± 0.89

effects of transfection via US and p-BLs on the biochemical values AST, ALT, ALP, and CK. AST and ALT were slightly increased in the group treated with p-BLs containing DDAB; however, those values returned to normal levels 48 h after the injection (data not shown). Therefore, it was assumed that transfection with p-BLs and US had little effect on liver function and muscle tissues. These results suggest that p-BLs containing DSDAP were the most effective as a US contrast agent and pDNA delivery tool compared to other BLs.

To determine the efficacy of the therapeutic effect, we transfected pDNA encoding bFGF into the ischemic hindlimb using US and p-BLs contained DSDAP. As a result, the mRNA levels of various angiogenic factors significantly increased, and the blood flow rate in the group treated with the bFGF gene also significantly improved compared to the control group, which was treated with saline or empty vector (Fig. 7). These results suggest that the combination of p-BLs containing DSDAP and US exposure could be a useful tool as a systemic gene delivery system and could be applicable to hindlimb ischemia therapy.

4. Discussion

Recently, the integration of diagnostic imaging capability with therapy is expected for clinical use, and theranostic agents have received a great deal of research interest [3]. US imaging is one of the most widespread diagnostic modalities used in clinics. Moreover, a combination of microbubbles and US has been proposed as a less invasive and tissue-specific intracellular delivery for

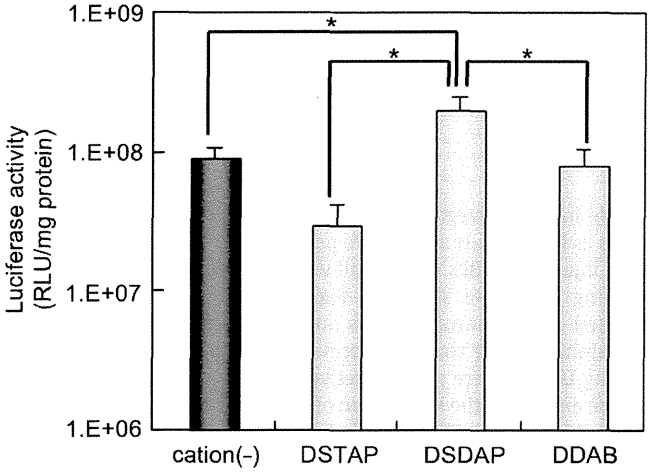

Fig. 4. Luciferase expression by cells transfected with pDNA using p-BLs and US. Luciferase expression in COS-7 cells transfected with pDNA (5 μg) using p-BLs (60 μg) and ultrasound (Frequency: 2 MHz, Duty: 50%, Burst rate: 2.0 Hz, Intensity: 2.0 W/cm^2, Time: 10 s) at 2 days post-transfection. All data represent the mean ± SD ($n = 4$).* indicates $P < 0.05$ using a one-way ANOVA with Tukey's post hoc test.

molecules such as dextran, pDNA, peptides, and siRNA both *in vitro* and *in vivo* [10–15,28,29]. However, the accessibility of microbubbles is restricted because of their size.

We previously developed nanosized pDNA-loaded BLs (p-BLs) and siRNA-loaded BLs (si-BLs) using DOTAP and demonstrated that the loading of nucleic acids onto BL improved the stability of the nucleic acids, and the effects of nucleic acids delivery were observed [21,22]. However, the gas retention ability of BLs containing DOTAP was lower than that of conventional BLs, and there remains room for improvement in their usability as a US contrast agent. It is known that short-chain and unsaturated fatty acids increase membrane fluidity [30]. DOTAP is unsaturated fatty acid and is thought to destabilize the membrane of BLs. In fact, the increased DOTAP content made it difficult to entrap the gas [22].

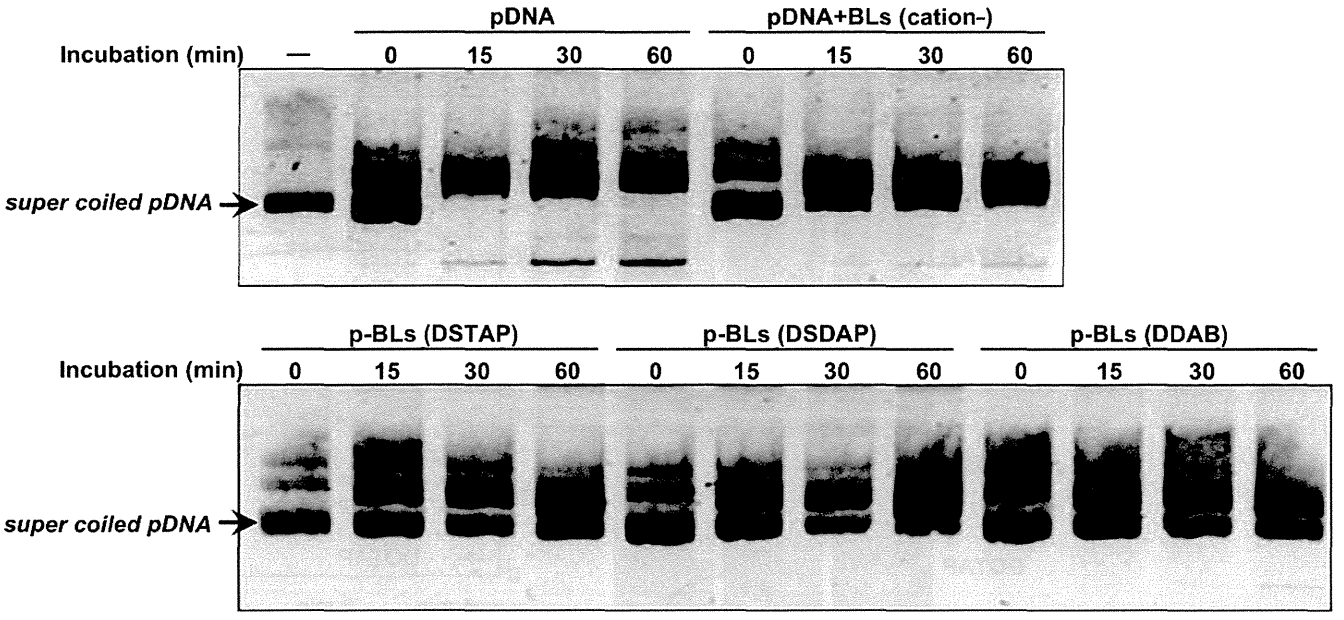

Fig. 3. Stability of pDNA in the presence of serum. Naked pDNA or p-BLs were subjected to 50% serum degradation at 37 °C for 15, 30, or 60 min and visualized via 1% agarose gel electrophoresis.

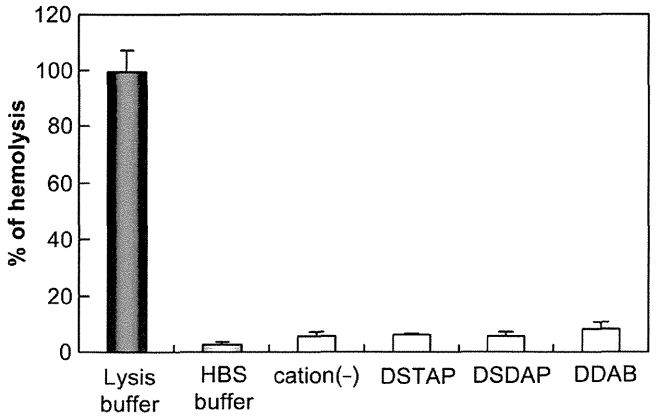

Fig. 5. Hemolysis test of BLs containing cationic lipids. Red blood cell suspensions were incubated with BLs or buffer for 4 h at 37 °C.

We therefore expected that p-BLs using other saturated cationic lipids would improve the stability of the liposomal membrane. Indeed, the three types of BLs tested here were more effective as a contrast agent compared to BLs containing DOTAP (Fig. 1). These results suggested that changing of the cationic lipid led to membrane stabilization and an improved gas retention ability.

The presence of nuclease in serum causes the degradation of DNA, which results in a loss of supercoiled content and leads to decreased transfection efficiency [31]. It has also been reported that the retention of the pDNA-supercoiled structure results in high transfection efficiency [32–34]. The proportion of pDNA loaded by BLs containing cationic lipid was 30–40%; however, loading onto the surface of BLs provided effective protection of pDNA against serum (Figs. 2 and 3). In contrast, free pDNA in solution or the mixture of pDNA and conventional BLs was not protected. Moreover, there were no significant changes in size and zeta potential after adding pDNA. These data suggested that pDNA was bound to the surface of BLs and that pDNA was protected by the fixed aqueous layer formed with PEG. Unexpectedly, there was no significant difference in the loading ratio and the pDNA protective effect among three types of BLs, although the acid dissociation constant (*pKa*) of DSDAP was low compared with that of DSTAP and DDAB. Furthermore, conventional BLs not containing cationic lipids also loaded small amounts of pDNA (data not shown). These results suggest that pDNA can be loaded not only by electrostatic interactions but also by the fixed aqueous layer formed with PEG. We also speculate that the stability of the membrane has some effect on the loading of pDNA. BLs with DSDAP might have a stable lipid membrane and could thus be useful both for US imaging and loading the pDNA.

The protective effects of the p-BLs tested here on pDNA were more pronounced than those of p-BLs containing DOTAP, although the pDNA loading ratios were roughly equivalent (data not shown). The difference in the protective effects might be due not only to the stability of membrane but also to the difference in cationic lipid content. BLs with DSTAP, DSDAP, or DDAB might be able to load pDNA more tightly than BLs with DOTAP. Therefore, the resistance to nuclease could improve. To maintain the integrity of pDNA in serum, pDNA should be stably held by BLs; however, US exposure should induce the cavitation of p-BLs, causing the pDNA to be released from the surface of BLs and transfected into cells. Prior to transfection experiments *in vivo*, we investigated the effect of gene delivery by p-BLs and US exposure *in vitro*. US exposure induced cavitation in all BLs and effective gene expression was observed (Fig. 4). Among them, the gene expression with p-BLs containing DSDAP was the highest. The difference in gene delivery effects

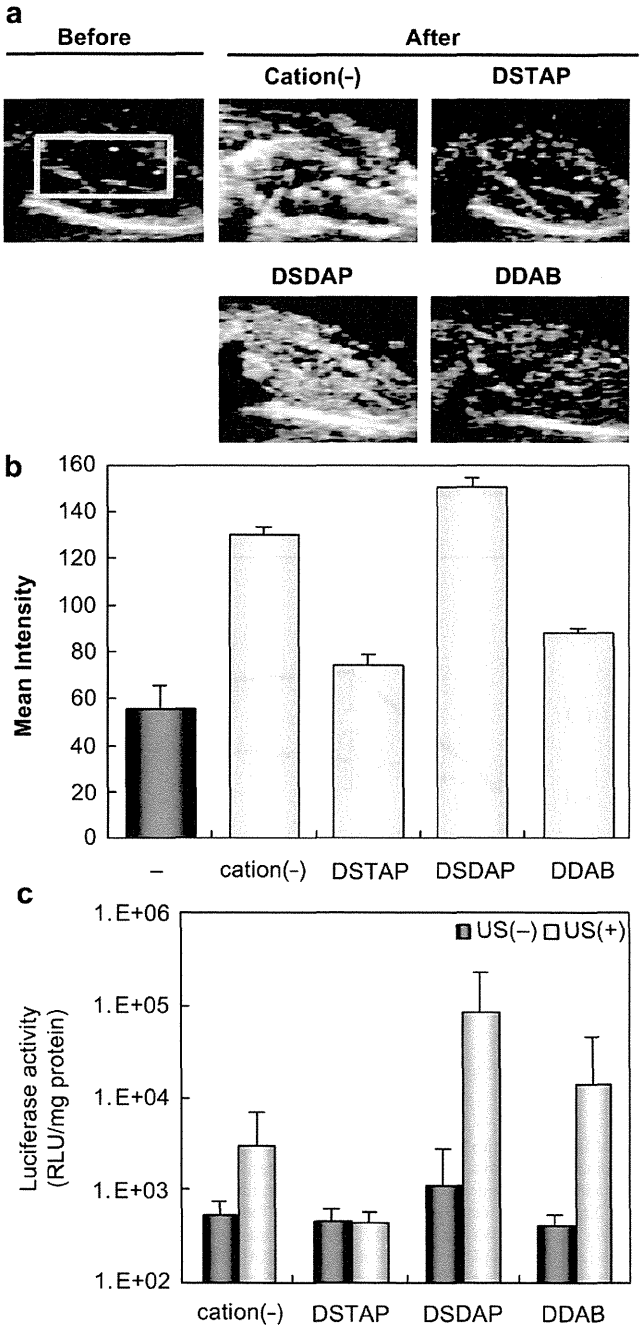

Fig. 6. (a) Ultrasonographic images of ischemic hindlimbs by various p-BLs (1 mg/mL, 200 μL) containing cationic lipids 30 s after injection. Yellow squares indicated the ROI. (b) Mean intensity of the pixels within the ROI. (c) Luciferase expression in ischemic muscle transfected with pDNA (50 μg) using p-BLs (1 mg/mL, 200 μL) and ultrasound (Frequency: 1 MHz, Duty: 50%, Burst rate: 2.0 Hz, Intensity: 1.0 W/cm^2, Time: 2 min) at 2 days post-transfection. (For interpretation of the references to color in this figure legend, the reader is referred to the web version of this article.)

might be due to the gas retention ability, the hardness of liposomal membrane, or the response to US. However, the stability of p-BLs *in vivo* could be important for reaching a target site via systemic injection.

We also examined whether p-BLs could be delivered to the ischemic hindlimb via microvessels using a US imaging system. The US echo signal was detected 5–10 s after the injection of p-BLs (Fig. 6a, b). The US imaging data for each BL demonstrated

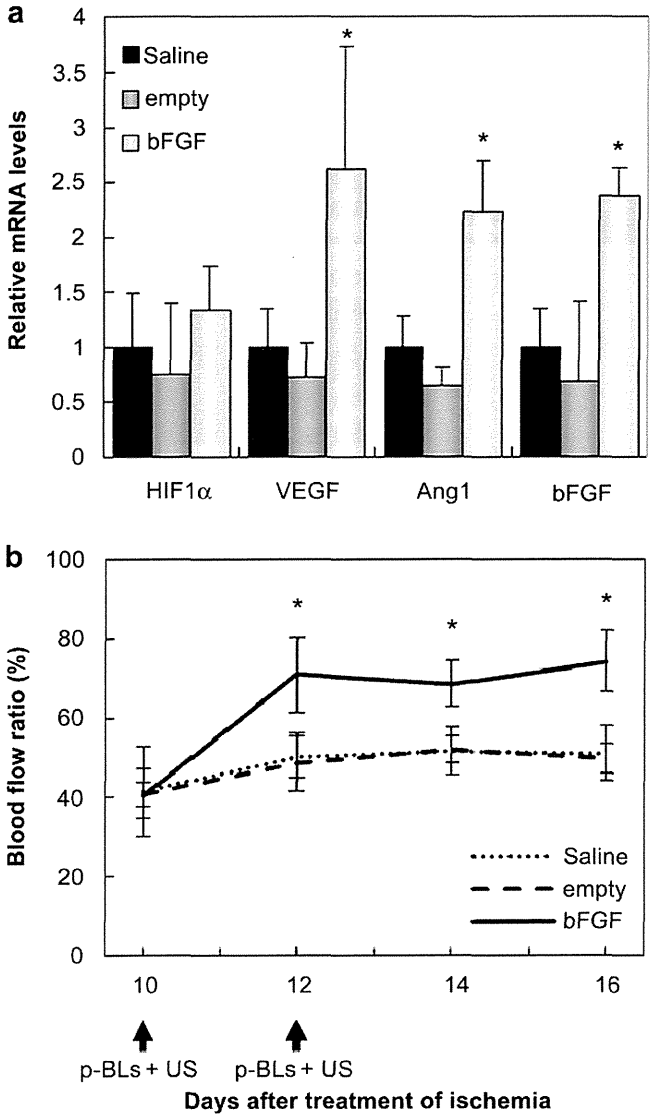

Fig. 7. The therapeutic effects of bFGF gene transfer by p-BLs and US exposure on mice with hindlimb ischemia. Ten days after femoral artery ligation, mice were treated with p-BLs and US (Frequency: 1 MHz, Duty: 50%, Burst rate: 2.0 Hz, Intensity: 1.0 W/cm^2, Time: 2 min), which mediated bFGF gene transfer. The treatment was administered via tail vein injection twice daily every 2 days to mice with hindlimb ischemia. We injected a solution of pDNA (pBLAST (empty) or pBLAST-bFGF, 50 μg) and BLs (200 μg). (a) The effect of bFGF gene transfer by p-BLs and US on mRNA expression of angiogenic genes. Four days after the second transfection, RNA was isolated from the thigh muscle and analyzed using real-time PCR. All data are reported as the mean ± SD (n = 5–6). (b) The effect of bFGF gene transfer using p-BLs and US on the recovery of blood flow. After the second transfection, blood flow was measured at 0–4 days using a laser Doppler blood flow meter. All data are reported as the mean ± SD (n = 3). * indicates $P < 0.05$ compared with the negative control.

a correlation between ischemic hindlimb and heart, as shown in Fig. 1 (data not shown). Therefore, the difference in the intensity shown in Fig. 6 among three types of p-BLs might be due to *in vivo* stability and p-BL accessibility, not to the US imaging ability of BLs. Indeed, the transfection effect was the most pronounced with the combination of US and p-BLs with DSDAP, which shown the highest intensity of the US echo signal (Fig. 6c). Furthermore, compared with conventional BLs, p-BLs with DSDAP were also more effective in systemic gene delivery, although the intensities of US imaging of ischemic hindlimbs were equally high. These results suggest that loading pDNA onto BLs containing cationic lipids could improve transfection efficiency via systemic injection. Indeed, the therapeutic effects were observed by transfecting the bFGF gene into ischemic hindlimb with US and p-BLs containing DSDAP (Fig. 7). We showed that BLs containing DSDAP were the most effective in US imaging and systemic gene delivery among three types of BLs.

To determine the feasibility of p-BLs, we attempted transfection into ischemic hindlimbs. However, we confirmed that there was no obvious difference in transfection effect between BLs and p-BLs in normal muscle tissue of the hindlimb (data not shown). This result suggests that tissue with thick veins could be transfected with US exposure given enough time, even when the mixture of pDNA and BLs is injected. In contrast, loading pDNA onto BLs could be important during transfection via microvessels or transfection into tissues with low blood flow. These findings suggest that p-BLs could be useful for gene delivery via microvessels not only to ischemic sites but also to deep tissues and tumor-inducing angiogenesis.

Recently, it has been reported that pDNA bound to cationic lipid-shelled microbubbles via electrostatic charge coupling led to an increase in gene transfection *in vitro* and *in vivo* [35–37]. However, the microbubbles used in these reports have a size of 1–5 μm. These microbubbles have difficulty penetrating deep into tissues. In contrast, nanosized p-BLs are a potentially superior carrier for extensive delivery into tissues. It is also expected that p-BLs will have widespread applications as delivery tools for various negatively charged molecules. Furthermore, we were able to improve the US imaging ability by changing the lipid composition. The BLs developed in this study could be effective tools for diagnosis and therapy. Microbubbles modified with antibodies that have a targeting function have recently been developed [38–40]. It would be easy to modify liposomes to add a targeting function. We have been successful in development of the targeted BLs modified with peptide [41]. Thus, the combination of molecularly targeted p-BLs and US may have strong potential to become theranostic agents and lead to beneficial clinical applications for various diseases.

5. Conclusion

In this study, we showed that three types of BLs could efficiently load pDNA and protect pDNA against deoxyribonuclease degradation. Furthermore, we demonstrated that the US imaging ability and transfection effect vary with the lipid component and that p-BLs containing DSDAP were the most effective. Indeed, in ischemic muscle, p-BLs with DSDAP could reach the ischemic site, be detected by diagnostic US, and deliver bFGF-expressing pDNA by therapeutic US, which led to the induction of angiogenic factors and improved blood flow. These results suggest that the combination of p-BLs and US exposure may be useful for US imaging and the delivery of pDNA to tissues or organs via systemic injection and may be applicable to a less invasive diagnostic and therapeutic system.

Acknowledgments

We are grateful to Prof. Katsuro Tachibana (Department of Anatomy, School of Medicine, Fukuoka University) for technical advice regarding the induction of cavitation with US, to Mr. Yasuharu Kato (School of Pharmacy, Tokyo University of Pharmacy and Life Sciences) for excellent technical assistance, and to Mr. Yasuhiko Hayakawa and Mr. Kosho Suzuki (NEPA GENE Co., Ltd.) for technical advice regarding US exposure. This study was supported by the Grant for Industrial Technology Research (04A05010) from the New Energy and Industrial Technology Development Organization (NEDO) of Japan, a Grant-in-Aid for Scientific Research (B) (20300179) from the Japan Society for the Promotion of Science,

and a Grant-in-Aid for Young Scientists (B) (21790164, 24790173) from the Japan Society for the Promotion of Science.

References

[1] Wagner V, Dullaart A, Bock AK, Zweck A. The emerging nanomedicine landscape. Nat Biotechnol 2006;24:1211–7.
[2] Kim BY, Rutka JT, Chan WC. Nanomedicine. N Engl J Med 2010;363:2434–43.
[3] Sumer B, Gao J. Theranostic nanomedicine for cancer. Nanomedicine 2008;3:137–40.
[4] Zhang L, Gu FX, Chan JM, Wang AZ, Langer RS, Farokhzad OC. Nanoparticles in medicine: therapeutic applications and developments. Clin Pharmacol Ther 2008;83:761–9.
[5] Derfus AM, Chen AA, Min DH, Ruoslahti E, Bhatia SN. Targeted quantum dot conjugates for siRNA delivery. Bioconjug Chem 2007;18:1391–6.
[6] Liong M, Lu J, Kovochich M, Xia T, Ruehm SG, Nel AE, et al. Multifunctional inorganic nanoparticles for imaging, targeting, and drug delivery. ACS Nano 2008;2:889–96.
[7] von Maltzahn G, Park JH, Agrawal A, Bandaru NK, Das SK, Sailor MJ, et al. Computationally guided photothermal tumor therapy using long-circulating gold nanorod antennas. Cancer Res 2009;69:3892–900.
[8] Ke H, Wang J, Dai Z, Jin Y, Qu E, Xing Z, et al. Gold-nanoshelled microcapsules: a theranostic agent for ultrasound contrast imaging and photothermal therapy. Angew Chem Int Ed Engl 2011;50:3017–21.
[9] Feshitan JA, Vlachos F, Sirsi SR, Konofagou EE, Borden MA. Theranostic Gd(III)-lipid microbubbles for MRI-guided focused ultrasound surgery. Biomaterials 2012;33:247–55.
[10] Taniyama Y, Tachibana K, Hiraoka K, Aoki M, Yamamoto S, Matsumoto K, et al. Development of safe and efficient novel nonviral gene transfer using ultrasound: enhancement of transfection efficiency of naked plasmid DNA in skeletal muscle. Gene Ther 2002;9:372–80.
[11] Taniyama Y, Tachibana K, Hiraoka K, Namba T, Yamasaki K, Hashiya N, et al. Local delivery of plasmid DNA into rat carotid artery using ultrasound. Circulation 2002;105:1233–9.
[12] Li T, Tachibana K, Kuroki M, Kuroki M. Gene transfer with echo-enhanced contrast agents: comparison between Albunex, Optison, and Levovist in mice–initial results. Radiology 2003;229:423–8.
[13] Unger EC, Porter T, Culp W, Labell R, Matsunaga T, Zutshi R. Therapeutic applications of lipid-coated microbubbles. Adv Drug Deliv Rev 2004;56:1291–314.
[14] Sonoda S, Tachibana K, Uchino E, Okubo A, Yamamoto M, Sakoda K, et al. Gene transfer to corneal epithelium and keratocytes mediated by ultrasound with microbubbles. Invest Ophthalmol Vis Sci 2006;47:558–64.
[15] Tsunoda S, Mazda O, Oda Y, Iida Y, Akabame S, Kishida T, et al. Sonoporation using microbubble BR14 promotes pDNA/siRNA transduction to murine heart. Biochem Biophys Res Commun 2005;336:118–27.
[16] Suzuki R, Takizawa T, Negishi Y, Hagisawa K, Tanaka K, Sawamura K, et al. Gene delivery by combination of novel liposomal bubbles with perfluoropropane and ultrasound. J Control Release 2007;117:130–6.
[17] Suzuki R, Takizawa T, Negishi Y, Utoguchi N, Sawamura K, Tanaka K, et al. Tumor specific ultrasound enhanced gene transfer *in vivo* with novel liposomal bubbles. J Control Release 2008;125:137–44.
[18] Suzuki R, Takizawa T, Negishi Y, Utoguchi N, Maruyama K. Effective gene delivery with novel liposomal bubbles and ultrasonic destruction technology. Int J Pharm 2008;354:49–55.
[19] Negishi Y, Endo Y, Fukuyama T, Suzuki R, Takizawa T, Omata D, et al. Delivery of siRNA into the cytoplasm by liposomal bubbles and ultrasound. J Control Release 2008;132:124–30.
[20] Negishi Y, Omata D, Iijima H, Takabayashi Y, Suzuki K, Endo Y, et al. Enhanced laminin-derived peptide AG73-mediated liposomal gene transfer by Bubble liposomes and ultrasound. Mol Pharm 2010;7:217–26.
[21] Negishi Y, Endo-Takahashi Y, Matsuki Y, Kato Y, Takagi N, Suzuki R, et al. Systemic delivery systems of angiogenic gene by novel Bubble liposomes containing cationic lipid and ultrasound exposure. Mol Pharm 2012;9:1834–40.
[22] Endo-Takahashi Y, Negishi Y, Kato Y, Suzuki R, Maruyama K, Aramaki Y. Efficient siRNA delivery using novel siRNA-loaded Bubble liposomes and ultrasound. Int J Pharm 2012;422:504–9.
[23] Haag P, Frauscher F, Gradl J, Seitz A, Schäfer G, Lindner JR, et al. Microbubble-enhanced ultrasound to deliver an antisense oligodeoxynucleotide targeting the human androgen receptor into prostate tumours. J Steroid Biochem Mol Biol 2006;102:103–13.
[24] Couffinhal T, Silver M, Zheng LP, Kearney M, Witzenbichler B, Isner JM. Mouse model of angiogenesis. Am J Pathol 1998;152:1667–79.
[25] Negishi Y, Matsuo K, Endo-Takahashi Y, Suzuki K, Matsuki Y, Takagi N, et al. Delivery of an angiogenic gene into ischemic muscle by novel Bubble liposomes followed by ultrasound exposure. Pharm Res 2011;28:712–9.
[26] Eliyahu H, Servel N, Domb AJ, Barenholz Y. Lipoplex-induced hemagglutination: potential involvement in intravenous gene delivery. Gene Ther 2002;9:850–8.
[27] Kurosaki T, Kitahara T, Kawakami S, Higuchi Y, Yamaguchi A, Nakagawa H, et al. Gamma-polyglutamic acid-coated vectors for effective and safe gene therapy. J Control Release 2010;142:404–10.
[28] Otani K, Yamahara K, Ohnishi S, Obata H, Kitamura S, Nagaya N. Nonviral delivery of siRNA into mesenchymal stem cells by a combination of ultrasound and microbubbles. J Control Release 2009;133:146–53.
[29] Du J, Shi QS, Sun Y, Liu PF, Zhu MJ, Du LF, et al. Enhanced delivery of monomethoxypoly(ethylene glycol)-poly(lactic-co-glycolic acid)-poly l-lysine nanoparticles loading platelet-derived growth factor BB small interfering RNA by ultrasound and/or microbubbles to rat retinal pigment epithelium cells. J Gene Med 2011;13:312–23.
[30] Lian T, Ho RJ. Trends and developments in liposome drug delivery systems. J Pharm Sci 2001;90:667–80.
[31] Kawabata K, Takakura Y, Hashida M. The fate of plasmid DNA after intravenous injection in mice: involvement of scavenger receptors in its hepatic uptake. Pharm Res 1995;12:825–30.
[32] Remaut K, Sanders NN, Fayazpour F, Demeester J, De Smedt SC. Influence of plasmid DNA topology on the transfection properties of DOTAP/DOPE lipoplexes. J Control Release 2006;115:335–43.
[33] Even-Chen S, Barenholz Y. DOTAP cationic liposomes prefer relaxed over supercoiled plasmids. Biochim Biophys Acta 2000;1509:176–88.
[34] Cherng JY, Schuurmans-Nieuwenbroek NM, Jiskoot W, Talsma H, Zuidam NJ, Hennink WE, et al. Effect of DNA topology on the transfection efficiency of poly((2-dimethylamino)ethyl methacrylate)-plasmid complexes. J Control Release 1999;60:343–53.
[35] Christiansen JP, French BA, Klibanov AL, Kaul S, Lindner JR. Targeted tissue transfection with ultrasound destruction of plasmid-bearing cationic microbubbles. Ultrasound Med Biol 2003;29:1759–67.
[36] Phillips LC, Klibanov AL, Bowles DK, Ragosta M, Hossack JA, Wamhoff BR. Focused *in vivo* delivery of plasmid DNA to the porcine vascular wall via intravascular ultrasound destruction of microbubbles. J Vasc Res 2010;47:270–4.
[37] Phillips LC, Klibanov AL, Wamhoff BR, Hossack JA. Targeted gene transfection from microbubbles into vascular smooth muscle cells using focused, ultrasound-mediated delivery. Ultrasound Med Biol 2010;36:1470–80.
[38] Leong-Poi H, Christiansen J, Heppner P, Lewis CW, Klibanov AL, Kaul S, et al. Assessment of endogenous and therapeutic arteriogenesis by contrast ultrasound molecular imaging of integrin expression. Circulation 2005;111:3248–54.
[39] Behm CZ, Kaufmann BA, Carr C, Lankford M, Sanders JM, Rose CE, et al. Molecular imaging of endothelial vascular cell adhesion molecule-1 expression and inflammatory cell recruitment during vasculogenesis and ischemia-mediated arteriogenesis. Circulation 2008;117:2902–11.
[40] Palmowski M, Huppert J, Ladewig G, Hauff P, Reinhardt M, Mueller MM, et al. Molecular profiling of angiogenesis with targeted ultrasound imaging: early assessment of antiangiogenic therapy effects. Mol Cancer Ther 2008;7:101–9.
[41] Negishi Y, Hamano N, Tsunoda Y, Oda Y, Choijamts B, Endo-Takahashi Y, et al. AG73-modified Bubble liposomes for targeted ultrasound imaging of tumor neovasculature. Biomaterials 2013;34:501–7.

molecular pharmaceutics

Brief Article

pubs.acs.org/molecularpharmaceutics

Bubble Liposomes and Ultrasound Enhance the Antitumor Effects of AG73 Liposomes Encapsulating Antitumor Agents

Nobuhito Hamano,[†,‡] Yoichi Negishi,*[,†,‡] Daiki Omata,[†] Yoko Takahashi,[†] Maya Manandhar,[†] Ryo Suzuki,[§] Kazuo Maruyama,[§] Motoyoshi Nomizu,[∥] and Yukihiko Aramaki[†]

[†]Department of Drug Delivery and Molecular Biopharmaceutics, School of Pharmacy, Tokyo University of Pharmacy and Life Sciences, Hachioji, Tokyo, Japan

[§]Laboratory of Drug and Gene Delivery, Faculty of Pharma Sciences, Teikyo University, Kaga, Itabashi-ku, Japan

[∥]Department of Clinical Biochemistry, School of Pharmacy, Tokyo University of Pharmacy and Life Sciences, Hachioji, Tokyo, Japan

Supporting Information

ABSTRACT: Encapsulating anticancer drugs in liposomes improves their therapeutic window by enhancing antitumor efficacy and reducing side effects. To devise more effective liposomal formulations for antitumor therapy, many research groups have tried to develop tumor-targeting liposomes with enhanced drug release. Previously, we developed doxorubicin (Dox)-encapsulated AG73 peptide-modified liposomes (AG73-Dox), which targeted cancer and endothelial cells, and ultrasound (US) imaging gas-entrapping liposomes, called "Bubble liposomes" (BLs). In this study, to enhance the antitumor effect of AG73-Dox, we combined AG73-Dox with BLs and US. First, to determine whether the addition of BLs and application of US could enhance the cytotoxicity of AG73-Dox, we evaluated the cytotoxicity of the combination of AG73-Dox with BLs and US. BLs and US enhanced cytotoxicity of AG73-Dox more than they enhanced nontargeted Dox-encapsulated liposomes. Next, we examined the intracellular behavior of Dox after treatment with BLs and US. The combination of AG73-Dox with BLs and US did not enhance cellular uptake of Dox, but it did promote drug release in the cytoplasm. To further elucidate the release of Dox in the cytoplasm, we blocked cellular uptake via endosomes at a low temperature. As a result, BLs and US did not have an enhanced drug-release effect until AG73-Dox was taken up into cells. Thus, the combination of AG73-Dox with BLs and US may be useful for cancer therapy as a dual-function drug delivery system with targeted and controlled release.

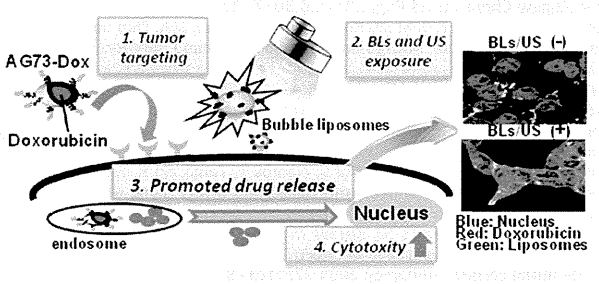

KEYWORDS: *liposomes, drug delivery, ultrasound, Bubble liposomes, AG73 peptide*

■ INTRODUCTION

Nanoparticle-based drug delivery systems, including liposomes, allow the targeting of anticancer drugs to tumors, and their development and optimization have been a major focus in the field of drug delivery. Encapsulating anticancer drugs in liposomes improves the therapeutic window by enhancing antitumor efficacy and reducing side effects.[1,2] To increase the antitumor effect of liposomal formulations, many research groups have tried to develop tumor-targeted liposomes and enhance drug release from such liposomes.[3−8] Previously, we developed doxorubicin (Dox)-encapsulated AG73 peptide-modified liposomes (AG73-Dox), which target cancer and endothelial cells.[9] The AG73 peptide is a ligand for syndecans, one of the major heparan sulfate-containing transmembrane proteoglycans.[10−12] Because syndecan-2 is highly expressed in various cancer cell lines, it makes it a potentially useful drug targeting moeity.[13−15] In this study, we focused on the use of ultrasound (US) to enhance the anticancer effects of a liposome treatment because it has been reported that US is effective at permeabilizing cellular membranes[19−22] and enhancing DNA transfection[16−18] and drug delivery. Furthermore, the combination of US exposure with microbubbles as a contrast agent during imaging improves drug delivery efficiency.[20,22−24] However, microbubbles have problems with size, stability, and targeting functionality. Therefore, we have developed US imaging gas-entrapping liposomes, called "Bubble liposomes" (BLs). We recently reported that BLs are suitable for gene delivery *in vitro* and *in vivo*.[25−31] Previously, we have reported that the combination of BL and US exposure could enhance liposomal gene transfection by promoting endosomal escape.[32−34] We hypothesized that the combination of AG73-Dox with BLs and US might be useful for cancer therapy. In this study, we examined whether BLs and US could enhance the antitumor effects of AG73-Dox and investigated the intracellular behavior of Dox after treatment with BLs and US.

Received: August 22, 2012
Revised: November 14, 2012
Accepted: December 4, 2012
Published: December 4, 2012

EXPERIMENTAL SECTION

Materials. Dipalmitoylphosphatidylcholine (DPPC), 1,2-distearoyl-*sn*-glycero-3-phosphocholine (DSPC), 1,2-distearoyl-phosphatidylethanolamine-methoxy-polyethyleneglycol (DSPE-PEG_{2000}-OMe), and 1,2-distearoyl-*sn*-glycero-3-phosphatidylethanolamine-polyethyleneglycol-maleimide (DSPE-PEG_{2000}-Mal) were purchased from NOF Corporation (Tokyo, Japan). Doxorubicin (Dox) was purchased from Sigma-Aldrich Co. (St. Louis, MO, USA). For cell culture, Dulbecco's modified Eagle's medium (DMEM) was purchased from Kohjin Bio Co. Ltd. (Tokyo, Japan). Fetal bovine serum (FBS) was purchased from Equitech Bio Inc. (Kerrville, TX, USA). All other materials were used without further purification.

Preparation of Dox-Encapsulating Liposomes. To prepare liposomes for encapsulating Dox, DSPC and DSPE-PEG_{2000}-OMe were mixed at a molar ratio of 94:6. Liposomes were prepared by a reverse-phase evaporation method, as described previously.[9] Briefly, all reagents were dissolved in 1:1 (v/v) chloroform/diisopropyl ether. Three hundred millimolar citrate buffer (pH 4.0) was then added to the lipid solution, and the mixture was sonicated and then evaporated at 65 °C. The organic solvent was completely removed, and the size of the liposomes was adjusted to approximately 150 nm using extruding equipment and sizing filters (pore sizes: 100 and 200 nm, Nuclepore Track-Etch Membrane, Whatman plc., U.K.). For fluorescent labeling of the lipid membrane, 1,2-dipalmitoyl-*sn*-glycero-3-phosphoethanolamine-*N*-(7-nitro-2-1,3-benzoxadiazol-4-yl) [triethylamine salt] (NBD-DPPE) was also added (1 mol % of total lipids). After size selection, the liposomes were passed through a 0.45 μm pore size filter (syringe filter, Asahi Techno Glass Co., Chiba, Japan) for sterilization. Then, the Dox-encapsulating liposomes were prepared by a remote loading method with a pH gradient.[35,36] In brief, liposomes were passed through a Sephadex G-50 (GE Healthcare UK Ltd., Buckinghamshire, England) spin column that was equilibrated with *N*-[2-hydroxyethyl]piperazine-*N*′-[2-ethanesulfonic acid] (HEPES)-buffered saline (HBS; 20 mM HEPES, 150 mM NaCl, pH 7.5) to exchange the external buffer. The eluted liposomes had a transmembrane pH gradient with pH 4.0 inside and pH 7.5 outside the liposomes. The eluted liposomes were incubated with Dox (at a Dox:lipid molar ratio of 1:5) at 65 °C for 30 min. To remove the unencapsulated Dox, the mixture was passed through a Sephadex G-50 spin column. The Dox-encapsulating liposomes (Dox-PEG) were stored at 4 °C until use. The efficiency for the remote loading of Dox into the liposomes was 90−95% with a drug:lipid molar ratio of 1:5.[9]

Preparation of Dox-Encapsulating AG73 Peptide-Modified Liposomes. The Cys-AG73 peptide (CGG-RKRLQVQLSIRT) and a scrambled Cys-AG73T control peptide (CGG-LQQRRSVLRTKI) were synthesized manually using the 9-fluorenylmethoxycarbonyl (Fmoc)-based solid-phase strategy. The peptides were prepared in the −COOH terminal amide form and purified by reverse-phase high-performance liquid chromatography. Dox-encapsulating liposomes composed of DSPC, DSPE-PEG_{2000}-OMe, and DSPE-PEG_{2000}-Mal at a molar ratio of 94:4:2 were prepared by a reverse-phase evaporation method and a remote loading method. For the preparation of Dox-encapsulating peptide-modified liposomes, peptides were added to liposomes and gently mixed as described previously.[9,37] In brief, for coupling, peptides at a molar ratio of 2-fold DSPE-PEG_{2000}-Mal were added to the Dox-encapsulating liposomes and the mixture was incubated for 24 h at 4 °C to conjugate the cysteine of the Cys-AG73 or Cys-AG73T peptide with the maleimide of the Dox-encapsulating liposomes using a thioether bond. The resulting peptide-conjugated Dox-encapsulating liposomes (AG73-Dox) were passed through a Sephadex G-50 spin column to remove any excess peptides. Peptide-conjugated Dox-encapsulating liposomes were modified with 6 mol % PEG and 2 mol % peptides. The mean particle diameters of Dox-PEG and AG73-Dox ranged from 130 to 170 nm.[9]

Preparation of BLs. To prepare BLs, DPPC and DSPE-PEG_{2000}-OMe were mixed in a molar ratio of 94:6. The liposomes were prepared by a reverse-phase evaporation method, as described previously.[28−31] BLs were prepared using liposomes and perfluoropropane gas (Takachiho Chemical Inc., Co., Ltd., Tokyo, Japan). First, 5 mL sterilized vials containing 2 mL of liposome suspension (lipid concentration 1 mg/mL) were filled with perfluoropropane gas, capped, and then pressurized with 7.5 mL of perfluoropropane gas. The vials were placed in a bath-type sonicator (42 kHz, 100 W, Bransonic 2510J-DTH, Branson Ultrasonics Co., Danbury, CT) for 5 min to form BLs. The mean size of the BLs was determined using light-scattering with a zeta potential/particle sizer (Nicomp 380ZLS, Santa Barbara, CA). The mean particle diameter of the BLs was approximately 500 nm.[28−31]

Cell Lines. 293T human embryonic kidney carcinoma cells that stably overexpressed syndecan-2 (293T-Syn2) were cultured in DMEM that was supplemented with 10% FBS, penicillin (100 U/mL), streptomycin (100 μg/mL), and puromycin (0.4 μg/mL) at 37 °C in a humidified 5% CO_2 atmosphere.

Cytotoxicity of AG73-Dox with BL and US Exposure. The cytotoxicity of AG73-Dox with BLs and US was determined using a WST assay. First, a 48-well plate was coated with type I collagen (Cellmatrix, Nitta Geratin Inc., Osaka, Japan). Two days before the experiments, 293T-Syn2 cells (1×10^4 cells/well) were seeded in the collagen-coated plate. The cells were treated with Dox-encapsulating liposomes ([Dox] = 3 μg/mL) for 4 h at 37 °C in 5% CO_2. After incubation, the cells were washed twice to remove the excess and unassociated liposomes, followed by addition of BLs (120 μg/mL). US was applied through a 6 mm diameter probe placed in the well (frequency, 2 MHz; duty cycle, 50%; burst rate, 2 Hz; intensity, 0.25−1.0 W/cm^2; time, 10 s). A sonopore 3000 (NEPA GENE, CO., Ltd., Chiba, Japan) was used to generate US. Cells were then cultured for 48 h at 37 °C in 5% CO_2. After incubation, 10 μL of cell-counting solution (WST-8, Dojindo Laboratories, Tokyo, Japan) was added to each well, and cells were further incubated for 2 h at 37 °C in 5% CO_2. Cell viability was assessed by measuring the absorbance at 450 nm with a reference absorbance at 650 nm (Infinite M1000, TECAN, Männedorf, Switzerland). Cell viability was calculated according to the following formula:

$$\text{cell viability (\%)} = \text{A450(sample} - \text{blank)} / \text{A450(control} - \text{blank)} \times 100$$

Flow Cytometry Analysis for the Intracellular Uptake of AG73-Dox with BL and US Exposure. The intracellular uptake of Dox was determined by flow cytometry analysis. Two days before the experiments, 293T-Syn2 cells (1×10^5 cells/

dx.doi.org/10.1021/mp300463h | *Mol. Pharmaceutics* 2013, 10, 774−779

well) were seeded in a 24-well plate. To examine the effect of BL and US exposure on cellular uptake of Dox, AG73-Dox liposomes ([Dox] = 20 μg/mL) were added to the cells and incubated for 4 h at 37 °C in 5% CO_2. After incubation, the cells were washed twice and BLs (120 μg/mL) were added. US exposure was then applied (frequency, 2 MHz; duty cycle, 50%; burst rate, 2 Hz; intensity, 0.25–1.0 W/cm^2; time, 10 s). Cells were then collected by trypsinization and washed with PBS three times. Fluorescence intensity was then measured by flow cytometry.

Confocal Microscopy Analysis. Two days before the experiments, 293T-Syn2 cells (5×10^4 cells/well) were seeded in a collagen coated 48-well plate. AG73-Dox ([Dox] = 10 μg/mL) was added to the cells and incubated for 4 h at 37 or 4 °C. Cells were then washed twice and BLs (120 μg/mL) were added. Then, US exposure was applied (frequency, 2 MHz; duty cycle, 50%; burst rate, 2 Hz; intensity, 0.25–1.0 W/cm^2; time, 10 s). The cells were subsequently incubated for 1 h and then fixed with 4% paraformaldehyde for 1 h at 4 °C. For nuclear staining, cells were treated with DAPI for 1 h. Fluorescence images of the cells were analyzed using an FV1000-D confocal microscope (OLYMPUS, Tokyo, Japan). The fluorescence intensity of images was calculated by using imaging analysis software (FLUOVIEW, OLYMPUS).

■ RESULTS AND DISCUSSION

We evaluated the cytotoxicity of AG73-Dox combined with BLs and US with a WST assay to examine whether the addition of BLs and application of US could enhance the cytotoxicity of AG73-Dox (Figure 1). Cells were treated with AG73-Dox for 4 h and washed twice to remove excess liposomes; then BLs were added and US was applied. As shown in Figure 1, cell viability was dependent on US intensity. Furthermore, BLs and US enhanced the cytotoxicity of AG73-Dox more than they enhanced the cytotoxicity of Dox-PEG. The viability of cells after treatment with BLs and US alone (in the absence of Dox-encapsulating liposomes) was not significantly diminished (cell viability was more than 80%). In a previous report, we showed that AG73-Dox could effectively target cancer cells, including 293T-Syn2.[9] These results suggest that AG73-Dox, in combination with BLs and US, could enhance the cytotoxicity of the encapsulated drug.

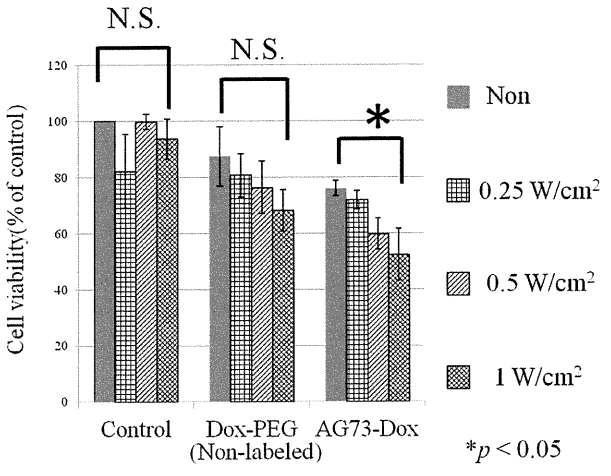

Figure 1. Cytotoxicity of AG73-Dox with BLs and US for 293T-Syn2 cells. The cells were incubated with Dox-encapsulated liposomes for 4 h at 37 °C ([Dox]: 3 μg/mL) . After incubation, cancer cells were washed and BLs were added. Then, the cells were exposed to US (frequency, 2 MHz; duty cycle, 50%; burst rate, 2 Hz; intensity, 0.25–1.0 W/cm^2; time, 10 s) and cultured for 48 h. Then, cell viability was measured using a WST assay. *p < 0.05. Data are shown as the mean ± SD.

Next, to examine the mechanism of enhanced cytotoxicity, we used flow cytometry to measure the cellular uptake of Dox after treatment with AG73-Dox with BLs and US. As shown in Figure 2, the fluorescence intensity did not change with US

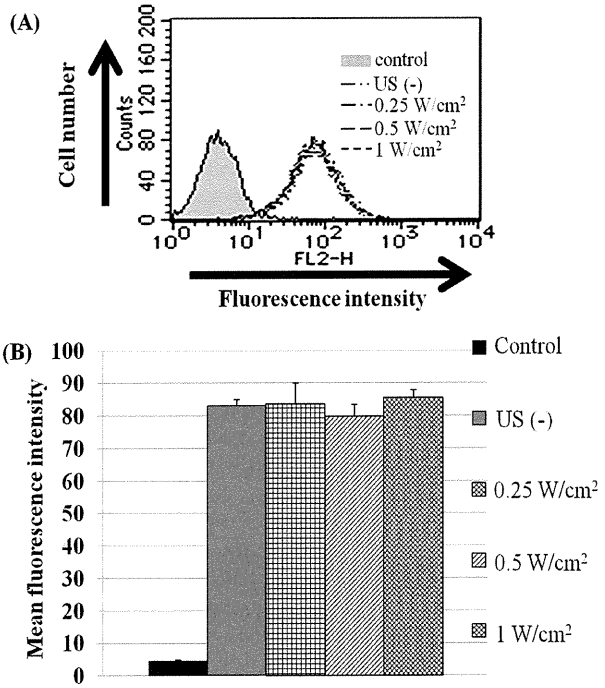

Figure 2. Cellular uptake of AG73-Dox with BLs and US on 293T-Syn2 cells. Cells were treated with AG73-Dox ([Dox] = 20 μg/mL) for 4 h at 37 °C. After incubation, cells were washed and BLs were added. Then, cells were exposed to US and fluorescence intensities were measured by flow cytometry. (A) Histogram analysis. (B) Mean fluorescence intensity analysis (n = 3).

exposure. These results suggest that cellular uptake of Dox is not related to US intensity. Additionally, although cellular uptake of Dox was low, even in the Dox-PEG treatment, the cellular uptake of Dox was identical in cells treated with AG73-Dox with BLs and US (data not shown). Moreover, to investigate the cellular mechanism for uptake of Dox, the intracellular localization of Dox was evaluated after treatment with AG73-Dox with BLs and US. As shown in Figure 3, when cells were treated first with AG73-Dox and subsequently treated with BLs and US, Dox was localized diffusely throughout the cytoplasm and its fluorescence was dependent on US intensity. These data suggest that the antitumor effects from treatment that combines AG73-Dox with both BLs and US may not result from enhanced cellular uptake of Dox but rather from enhanced drug release in the cytoplasm.

To further investigate the diffusion of Dox in the cytoplasm, we blocked cellular uptake by culturing cells at low temperature. As shown in Figure 4, the intracellular distribution of Dox in the cytoplasm of cells treated with AG73-Dox at 37 °C

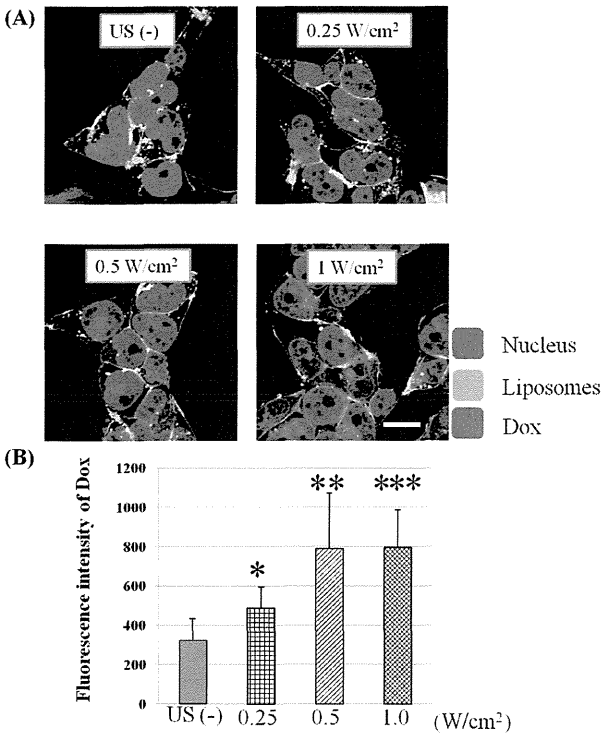

Figure 3. Effect of BL and US exposure on localization of Doxorubicin and liposomes. 293T-Syn2 cells incubated with AG73-Dox ([Dox] = 10 μg/mL) for 4 h at 37 °C. After incubation, cells were washed and BLs were added. Then, the cells were exposed to US. After incubation for 1 h, the cells were fixed. The cells were treated with DAPI (blue) for nuclear staining. (A) Confocal laser scanning microscopy (CLSM) analysis. Blue: DAPI. Red: Dox. Green: liposomes. Scale bars: 20 μm. (B) Fluorescence intensity of Dox. Data are shown as the mean ± SD (n = 8). *p < 0.05, **p < 0.01, ***p < 0.005 compared with US (−).

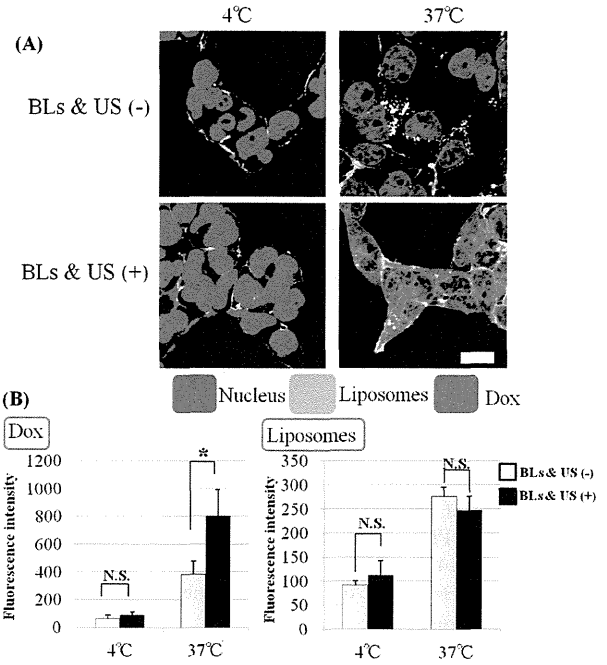

Figure 4. Effect of BLs and US on endosomal uptake. 293T-Syn2 cells were incubated with AG73-Dox ([Dox] = 10 μg/mL) for 4 h at 37 or 4 °C. After incubation, cells were washed and BLs were added. Then, the cells were exposed to US (frequency, 2 MHz; duty cycle, 50%; burst rate, 2.0 Hz; intensity, 1.0 W/cm^2; time, 10 s). After incubation for 1 h, the cells were fixed and stained with DAPI (blue) for nuclear staining. (A) Confocal laser scanning microscopy (CLSM) analysis. Blue: DAPI. Red: Dox. Green: liposomes. Scale bars: 20 μm. (B) Fluorescence intensity of Dox and liposomes. Data are shown as the means ± SD (n = 6) . *p < 0.005 compared with BLs and US (−).

was more widespread after treatment with BLs and US. On the other hand, the distribution of Dox in the cytoplasm after the same liposomal treatment at 4 °C was not increased by BLs and US. We hypothesized that this was because the AG73-Dox could not be endocytosed under the low temperature condition (Figure 4). This idea is further supported by comparing the fluorescent distributions of Dox and liposomes. While the fluorescence intensity of Dox in the cytoplasm was enhanced by BLs and US, fluorescence intensity of liposomes did not change (Figure 4 B). These results suggest that BLs and US do not affect the uptake of liposomes into the cytoplasm but rather enhance the effects of Dox by increasing drug release once the AG73-Dox is already in the cytoplasm. Taken together, these results suggest the following treatment mechanism: (1) AG73-Dox is selectively endocytosed by cells and partially trapped within endosomes (Figure S1 in the Supporting Information); (2) Dox is released from AG73-Dox inside the endosomes, and release is enhanced by application of BLs and US. Previously, we have reported that the combination of BL and US exposure could enhance liposomal gene transfection by promoting endosomal escape.[32−34] The endosomal escape of AG73 peptide-modified liposomes induced by BL and US exposure was significantly suppressed in the absence of Ca^{2+} or ATP, suggesting that these cofactors are necessary to facilitate drug release.[34] In addition, the combination of BLs and US did not increase the release of Dox from liposomes (Figure S2 in the Supporting Information). It could be suggested that the combination of BL and US exposure promoted endosomal escape of Dox, leading to dispersed Dox in cytoplasm. Consequently, this technique that enhances intracellular delivery of AG73-Dox via ligand-specific endocytosis and intracellular release via BLs and US can cause significant cancer cell cytotoxicity. BLs and US may also be useful for enhancing drug release in other targeting carriers modified with ligands (e.g., antibodies,[3−5] folate,[38] RGD peptide,[39] or transferrin[40]).

Recently, high-intensity focused ultrasound (HIFU) has attracted attention as a noninvasive technique for the treatment of solid tumors.[41,42] This method involves the ablation of cancerous tissue via heat and cavitation. Anticancer agents are administered before, during, or after HIFU exposure. Moreover, the combination of microbubbles with HIFU can enhance the therapeutic effects of HIFU.[43−45] Therefore, it would be anticipated that the combination of a targeting agent, such as AG73-Dox, with BLs and HIFU would enhance the effects of treatment and make this a useful method for cancer therapy.

In this study, we observed cancer cell cytotoxicity caused by the combination of AG73-Dox with BLs and US. The uptake of AG73-Dox via endosomes, followed by the application of both BLs and US, enhanced cytotoxicity compared to the combination of PEG-Dox with BLs and US. We next examined the intracellular behavior of Dox after treatment with BLs and US. In this experiment, the combined treatment of AG73-Dox with BLs and US did not enhance cellular uptake of Dox, but

dx.doi.org/10.1021/mp300463h | Mol. Pharmaceutics 2013, 10, 774−779

rather promoted drug release into the cytoplasm. To further investigate the release mechanism of Dox in the cytoplasm, we blocked cellular uptake of Dox using a low temperature treatment. Under the low temperature condition, treatment with BLs and US did not result in a drug release-enhancing effect until AG73-Dox was endocytosed by the cells. These results suggest that the combination of AG73-Dox with BLs and US is useful for cancer therapy as a dual-function drug delivery system with targeted and controlled release.

■ ASSOCIATED CONTENT

Supporting Information

Additional experimental details and figures as discussed in the text. This material is available free of charge via the Internet at http://pubs.acs.org.

■ AUTHOR INFORMATION

Corresponding Author

*Department of Drug Delivery and Molecular Biopharmaceutics, School of Pharmacy, Tokyo University of Pharmacy and Life Sciences, 1432-1 Horinouchi, Hachioji, Tokyo 192-0392, Japan. Tel/fax: +81 42 676 3183. E-mail: negishi@toyaku.ac.jp.

Author Contributions

‡The first two authors contributed equally to this work.

Notes

The authors declare no competing financial interest.

■ ACKNOWLEDGMENTS

We are grateful to Prof. Katsuro Tachibana (Department of Anatomy, School of Medicine, Fukuoka University) for technical advice regarding the induction of cavitation with US and to Mr. Yasuhiko Hayakawa and Mr. Kosho Suzuki (NEPA GENE CO., LTD.) for technical advice regarding exposure to US. This study was supported by an Industrial Technology Research Grant (04A05010) from the New Energy and Industrial Technology Development Organization (NEDO) of Japan and a Grant-in-Aid for Scientific Research (B) (20300179) from the Japan Society for the Promotion of Science.

■ REFERENCES

(1) Perez, A. T.; Domenech, G. H.; Frankel, C.; Vogel, C. L. Pegylated liposomal doxorubicin (Doxil) for metastatic breast cancer: the Cancer Research Network, Inc., experience. *Cancer Invest.* **2002**, *20* (Suppl. 2), 22–29.

(2) Allen, T. M.; Cullis, P. R. Drug delivery systems: entering the mainstream. *Science* **2004**, *303* (5665), 1818–1822.

(3) Lukyanov, A. N.; Elbayoumi, T. A.; Chakilam, A. R.; Torchilin, V. P. Tumor-targeted liposomes: doxorubicin-loaded long-circulating liposomes modified with anti-cancer antibody. *J. Controlled Release* **2004**, *100* (1), 135–144.

(4) Pan, X. G.; Wu, G.; Yang, W. L.; Barth, R. F.; Tjarks, W.; Lee, R. J. Synthesis of cetuximab-immunoliposomes via a cholesterol-based membrane anchor for targeting of EGFR. *Bioconjugate Chem.* **2007**, *18* (1), 101–108.

(5) Hatakeyama, H.; Akita, H.; Ishida, E.; Hashimoto, K.; Kobayashi, H.; Aoki, T.; Yasuda, J.; Obata, K.; Kikuchi, H.; Ishida, T.; Kiwada, H.; Harashima, H. Tumor targeting of doxorubicin by anti-MT1-MMP antibody-modified PEG liposomes. *Int. J. Pharm.* **2007**, *342* (1–2), 194–200.

(6) Li, S. D.; Huang, L. Pharmacokinetics and biodistribution of nanoparticles. *Mol. Pharmaceutics* **2008**, *5* (4), 496–504.

(7) Tagami, T.; Ernsting, J. M.; Li, S. D. Efficient tumor regression by a single and low dose treatment with a novel and enhanced formulation of thermosensitive liposomal doxorubicin. *J. Controlled Release* **2011**, *152* (2), 303–309.

(8) Zheng, Y.; Liu, X.; Samoshina, N. M.; Chertkov, V. A.; Franz, A. H.; Guo, X.; Samoshin, V. V. Fliposomes: pH-controlled release from liposomes containing new trans-2-morpholinocyclohexanol-based amphiphiles that perform a conformational flip and trigger an instant cargo release upon acidification. *Nat. Prod. Commun.* **2012**, *7* (3), 353–358.

(9) Negishi, Y.; Hamano, N.; Omata, D.; Fujisawa, A.; Manandhar, M.; Nomizu, M.; Aramaki, Y. Effect of doxorubicin-encupsulating AG73 peptide-modified liposomes on tumor selectively and cytotoxity. *Results Pharma Sci.* **2011**, *1* (1), 68–75.

(10) Carey, D. J. Syndecans: multifunctional cell-surface co-receptors. *Biochem. J.* **1997**, *327* (Part 1), 1–16.

(11) Hoffman, M, P.; Nomizu, M.; Roque, E.; Lee, S.; Jung, D. W.; Yamada, Y.; Kleinman, H, K. Laminin-1 and laminin-2 G-domain synthetic peptides bind syndecan-1 and are involved in acinar formation of a human submandibular gland cell line. *J. Biol. Chem.* **1998**, *273* (44), 28633–28641.

(12) Suzuki, N.; Ichikawa, N.; Kasai, S.; Yamada, M.; Nishi, N.; Morioka, H.; Yamashita, H.; Kitagawa, Y.; Utani, A.; Hoffman, M, P.; Nomizu, M. Syndecan binding sites in the laminin alpha1chain G domain. *Biochemistry* **2003**, *42* (43), 12625–12633.

(13) Han, I.; Park, H.; Oh, E. S. New insights into syndecan-2 expression and tumourigenic activity in colon carcinoma cells. *J. Mol. Histol.* **2004**, *35* (3), 319–326.

(14) Tkachenko, E.; Rhodes, J, M.; Simons, M. Syndecans: new kids on the signaling block. *Circ. Res.* **2005**, *96* (5), 488–500.

(15) Essner, J. J.; Chen, E.; Ekker, S. C. Syndecan-2. *Int. J. Biochem. Cell Biol.* **2006**, *38* (2), 152–156.

(16) Liu, J.; Lewis, T. N.; Prausnitz, M. R. Non-invasive assessment and control of ultrasound-mediated membrane permeabilization. *Pharm. Res.* **1998**, *15* (6), 918–924.

(17) Shohet, R. V.; Chen, S.; Zhou, Y. T.; Wang, Z.; Meidell, R. S.; Unger, R. H.; Grayburn, P. A. Echocardiographic destruction of albumin microbubbles directs gene delivery to the myocardium. *Circulation* **2000**, *101* (22), 2554–2556.

(18) Cochran, S. A.; Prausnitz, M. R. Sonoluminescence as an indicator of cell membrane disruption by acoustic cavitation. *Ultrasound Med. Biol.* **2001**, *27* (6), 841–850.

(19) Unger, E. C.; McCreery, T. P.; Sweitzer, R. H.; Caldwell, V. E.; Wu, Y. Acoustically active lipospheres containing paclitaxel: a new therapeutic ultrasound contrast agent. *Invest. Radiol.* **1998**, *33* (12), 886–892.

(20) Unger, E. C.; Hersh, E.; Vannan, M.; Matsunaga, T. O.; McCreery, T. Local drug and gene delivery through microbubbles. *Prog. Cardiovasc. Dis.* **2001**, *44* (1), 45–54.

(21) Tachibana, K.; Feril, L. B., Jr.; Ikeda-Dantsuji, Y. Sonodynamic therapy. *Ultrasonics* **2008**, *48* (4), 253–259.

(22) Feril, L. B., Jr.; Tachibana, K. Use of ultrasound in drug delivery systems: emphasis on experimental methodology and mechanisms. *Int. J. Hyperthermia* **2012**, *28* (4), 282–289.

(23) Matsuo, M.; Yamaguchi, K.; Feril, L. B., Jr.; Endo, H.; Ogawa, K.; Tachibana, K.; Nakayama, J. Synergistic inhibition of malignant melanoma proliferation by melphalan combined with ultrasound and microbubbles. *Ultrason. Sonochem.* **2011**, *18* (5), 1218–1224.

(24) O'Reilly, M. A.; Hynynen, K. Ultrasound enhanced drug delivery to the brain and central nervous system. *Int. J. Hyperthermia* **2012**, *28* (4), 386–396.

(25) Suzuki, R.; Takizawa, T.; Negishi, Y.; Hagisawa, K.; Tanaka, K.; Sawamura, K.; Utoguchi, N.; Nishioka, T.; Maruyama, K. Gene delivery by combination of novel liposomal bubbles with perfluoropropane and ultrasound. *J. Controlled Release* **2007**, *117* (1), 130–136.

(26) Suzuki, R.; Takizawa, T.; Negishi, Y.; Utoguchi, N.; Maruyama, K. Effective gene delivery with novel liposomal bubbles and ultrasonic destruction technology. *Int. J. Pharm.* **2008**, *354* (1–2), 49–55.

(27) Suzuki, R.; Takizawa, T.; Negishi, Y.; Utoguchi, N.; Sawamura, K.; Tanaka, K.; Namai, E.; Oda, Y.; Matsumura, Y.; Maruyama, K.

Tumor specific ultrasound enhanced gene transfer in vivo with novel liposomal bubbles. *J. Controlled Release* **2008**, *125* (2), 137–144.
(28) Negishi, Y.; Matsuo, K.; Endo-Takahashi, Y.; Suzuki, K.; Matsuki, Y.; Takagi, N.; Suzuki, R.; Maruyama, K.; Aramaki, Y. Delivery of an angiogenic gene into ischemic muscle by novel bubble liposomes followed by ultrasound exposure. *Pharm. Res.* **2011**, *28* (4), 712–719.
(29) Negishi, Y.; Tsunoda, Y.; Endo-Takahashi, Y.; Oda, Y.; Suzuki, R.; Maruyama, K.; Yamamoto, M.; Aramaki, Y. Local gene delivery system by bubble liposomes and ultrasound exposure into joint synovium. *J. Drug Delivery* **2011**, *2011*, 203986.
(30) Endo-Takahashi, Y.; Negishi, Y.; Kato, Y.; Suzuki, R.; Maruyama, K.; Aramaki, Y. Efficient siRNA delivery using novel siRNA-loaded Bubble liposomes and ultrasound. *Int. J. Pharm.* **2012**, *422* (1–2), 504–509.
(31) Negishi, Y.; Endo-Takahashi, Y.; Matsuki, Y.; Kato, Y.; Takagi, N.; Suzuki, R.; Maruyama, K.; Aramaki, Y. Systemic delivery systems of angiogenic gene by novel bubble liposomes containing cationic lipid and ultrasound exposure. *Mol. Pharmaceutics* **2012**, *9* (6), 1834–1840.
(32) Omata, D.; Negishi, Y.; Hagiwara, S.; Yamamura, S.; Endo-Takahashi, Y.; Suzuki, R.; Maruyama, K.; Nomizu, M.; Aramaki, Y. Bubble liposomes and ultrasound promoted endosomal escape of TAT-PEG liposomes as gene delivery carriers. *Mol. Pharmaceutics* **2011**, *8* (6), 2416–2423.
(33) Omata, D.; Negishi, Y.; Hagiwara, S.; Yamamura, S.; Endo-Takahashi, Y.; Suzuki, R.; Maruyama, K.; Aramaki, Y. Enhanced gene delivery using Bubble liposomes and ultrasound for folate-PEG liposomes. *J. Drug Targeting* **2012**, *20* (4), 355–363.
(34) Omata, D.; Negishi, Y.; Yamamura, S.; Hagiwara, S.; Endo-Takahashi, Y.; Suzuki, R.; Maruyama, K.; Nomizu, M.; Aramaki, Y. Involvement of Ca^{2+} and ATP in enhanced gene delivery by bubble liposomes and ultrasound exposure. *Mol. Pharmaceutics* **2012**, *9* (4), 1017–1023.
(35) Dos Santos, N.; Cox, K. A.; McKenzie, C. A.; van Baarda, F.; Gallagher, R. C.; Karlsson, G.; Edwards, K.; Mayer, L. D.; Allen, C.; Bally, M. B. pH gradient loading of anthracyclines into cholesterol-free liposomes: enhancing drug loading rates through use of ethanol. *Biochim. Biophys. Acta* **2004**, *1661* (1), 47–60.
(36) Negussie, A. H.; Miller, J. L.; Reddy, G.; Drake, S. K.; Wood, B. J.; Dreher, M. R. Synthesis and in vitro evaluation of cyclic NGR peptide targeted thermally sensitive liposome. *J. Controlled Release* **2010**, *143* (2), 265–273.
(37) Negishi, Y.; Omata, D.; Iijima, H.; Takabayashi, Y.; Suzuki, K.; Endo, Y.; Suzuki, R.; Maruyama, K.; Nomizu, M.; Aramaki, Y. Enhanced laminin-derived peptide AG73-mediated liposomal gene transfer by bubble liposomesand ultrasound. *Mol. Pharmaceutics* **2010**, *7* (1), 217–226.
(38) Gabizon, A.; Shmeeda, H.; Horowitz, A. T.; Zalipsky, S. Tumor cell targeting of liposome-entrapped drugs with phospholipid-anchored folic acid-PEG conjugates. *Adv. Drug Delivery Rev.* **2004**, *56* (8), 1177–1192.
(39) Xiong, X. B.; Huang, Y.; Lu, W. L.; Zhang, X.; Zhang, H.; Nagai, T.; Zhang, Q. Enhanced intracellular delivery and improved antitumor efficacy of doxorubicin by sterically stabilized liposomes modified with a synthetic RGD mimetic. *J. Controlled Release* **2005**, *107* (2), 262–275.
(40) Suzuki, R.; Takizawa, T.; Kuwata, Y.; Mutoh, M.; Ishiguro, N.; Utoguchi, N.; Shinohara, A.; Eriguchi, M.; Yanagie, H.; Maruyama, K. Effective anti-tumor activity of oxaliplatin encapsulated intransferrin-PEG-liposome. *Int. J. Pharm.* **2008**, *346* (1–2), 143–150.
(41) Li, C.; Zhang, W.; Fan, W.; Huang, J.; Zhang, F.; Wu, P. Noninvasive treatment of malignant bone tumors using high-intensity focused ultrasound. *Cancer* **2010**, *116* (16), 3934–3942.
(42) Chen, W.; Zhu, H.; Zhang, L.; Li, K.; Su, H.; Jin, C.; Zhou, K.; Bai, J.; Wu, F.; Wang, Z. Primary bone malignancy: effective treatment with high-intensity focused ultrasound ablation. *Radiology* **2010**, *255* (3), 967–978.
(43) Li, Q.; Du, J.; Yu, M.; He, G.; Luo, W.; Li, H.; Zhou, X. Transmission electron microscopy of VX2 liver tumors after high-intensity focused ultrasound ablation enhanced withSonoVue. *Adv. Ther.* **2009**, *26* (1), 117–125.
(44) Luo, W.; Zhou, X.; Yu, M.; He, G.; Zheng, X.; Li, Q.; Liu, Q.; Han, Z.; Zhang, J.; Qian, Y. Ablation of high-intensity focused ultrasound assisted with SonoVue on Rabbit VX2 liver tumors: sequential findings with histopathology, immunohistochemistry, and enzyme histochemistry. *Ann. Surg. Oncol.* **2009**, *16* (8), 2359–2368.
(45) Chung, D. J.; Cho, S. H.; Lee, J. M.; Hahn, S. T. Effect of microbubble contrast agent during high intensity focused ultrasound ablation on rabbit liver in vivo. *Eur. J. Radiol.* **2012**, *81* (4), e519–523.

Biomaterials 34 (2013) 501–507

Contents lists available at SciVerse ScienceDirect

Biomaterials

journal homepage: www.elsevier.com/locate/biomaterials

AG73-modified Bubble liposomes for targeted ultrasound imaging of tumor neovasculature

Yoichi Negishi [a,*,1], Nobuhito Hamano [a,1], Yuka Tsunoda [a,1], Yusuke Oda [b], Batsuren Choijamts [c], Yoko Endo-Takahashi [a], Daiki Omata [b], Ryo Suzuki [b], Kazuo Maruyama [b], Motoyoshi Nomizu [d], Makoto Emoto [c], Yukihiko Aramaki [a]

[a] Department of Drug Delivery and Molecular Biopharmaceutics, School of Pharmacy, Tokyo University of Pharmacy and Life Sciences, 1432-1 Horinouchi, Hachioji, Tokyo 192-0392, Japan
[b] Laboratory of Drug and Gene Delivery, Faculty of Pharma-sciences, Teikyo University, Japan
[c] Division of Gynecology, Center for Preventive Medicine Fukuoka Sanno Hospital, International University of Health and Welfare, Fukuoka, Japan
[d] Department of Clinical Biochemistry, School of Pharmacy, Tokyo University of Pharmacy and Life Sciences, Hachioji, Tokyo, Japan

ARTICLE INFO

Article history:
Received 2 August 2012
Accepted 23 September 2012
Available online 22 October 2012

Keywords:
Ultrasound imaging
Contrast agent
Microbubble
Tumor targeting peptide

ABSTRACT

Ultrasound imaging is a widely used imaging technique. The use of contrast agents has become an indispensible part of clinical ultrasound imaging, and molecular imaging via ultrasound has recently attracted significant attention. We recently reported that "Bubble liposomes" (BLs) encapsulating US imaging gas liposomes were suitable for ultrasound imaging and gene delivery. The 12 amino acid AG73 peptide derived from the laminin α1 chain is a ligand for syndecans, and syndecan-2 is highly expressed in blood vessels. In this study, we prepared AG73 peptide-modified BLs (AG73-BLs) and assessed their specific attachment and ultrasound imaging ability for blood vessels *in vitro* and *in vivo*. First, we assessed the specific attachment of AG73-BLs *in vitro*, using flow cytometry and microscopy. AG73-BLs showed specific attachment compared with non-labeled or control peptide-modified BLs. Next, we examined ultrasound imaging in tumor-bearing mice. When BLs were administered, contrast imaging of AG73-BLs was sustainable for up to 4 min, while contrast imaging of non-labeled BLs was not observed. Thus, it is suggested that AG73-BLs may become useful ultrasound contrast agents in the clinic for diagnosis based on ultrasound imaging.

1. Introduction

Ultrasound (US) imaging is a widely used diagnostic technique which offers high spatial resolution, allows for real-time imaging, and combines the advantages of noninvasiveness with the lack of ionizing radiation, easy access to the public, and low cost [1,2]. US contrast agents are gas-filled, echogenic microbubbles that remain exclusively in the vascular compartment [2]. The application of microbubbles has become an indispensible part of clinical US imaging [3], and molecular imaging via ultrasound has recently attracted significant attention [4]. Microbubbles help to enhance the specificity and sensitivity of imaging for various types of diseases, especially with tumors [5]. Moreover, ultrasound has been made more sensitive and can detect disease-associated endothelial receptors, a technique known as molecular ultrasound imaging [2,6–8]. It should be noted that compared with contrast agents for computed tomography (CT) and magnetic resonance imaging (MRI), microbubbles are much larger (2–8 μm) [9].

Polyethyleneglycol (PEG)-modified liposomes have excellent biocompatibility, stability, and a long circulation time and can be easily prepared in a variety of sizes and modified to add a targeting function. For these reasons, they have been widely used as carriers of drugs, antigens, and genes [10–14]. Therefore, PEG-liposomes containing a US imaging gas could be used as contrast agents. We recently reported that "Bubble liposomes" (BLs) were suitable for US imaging and gene delivery [15–21]. However, the imaging ability of BLs is only validated *in vitro*, and to improve the ability of US contrast agent, it is necessary to remodel BLs for molecular targeting.

Angiogenesis, the formation of new blood vessels, is promoted early in tumorigenesis and is a critical determinant of tumor growth, invasion, and metastatic potential [22]. Growth and metastasis of solid tumors requires induction of angiogenesis, the

* Corresponding author. Tel./fax: +81 42 676 3183.
E-mail address: negishi@toyaku.ac.jp (Y. Negishi).
[1] These authors contributed equally to this work.

0142-9612/$ – see front matter © 2012 Elsevier Ltd. All rights reserved.
http://dx.doi.org/10.1016/j.biomaterials.2012.09.056

creation and remodeling of new blood vessels from a pre-existing vascular network, to ensure the delivery of oxygen, nutrients, and growth factors to rapidly dividing transformed cells. Without the ability to induce angiogenesis, most neoplasms would fail to grow larger than 2 mm in diameter or metastasize [23].

Here, we have focused on AG73, which is a 12-amino-acid synthetic peptide derived from the globular domain of the laminin α1 chain. AG73 peptide is a ligand for syndecans, a major heparan sulfate-containing transmembrane proteoglycans [24–26]. Moreover, syndecan-2 is highly expressed in neovascular vessels [27–30]. Therefore, we developed AG73 peptide-modified Bubble liposomes (AG73-BLs) as neovascular-targeting BLs to enhance the contrast image.

We prepared AG73-BLs and assessed the specific attachment of AG73-BLs to blood vessels *in vitro* and *in vivo*. Furthermore, we examined the US imaging ability of these AG73-BLs.

2. Materials and methods

2.1. Materials

Dipalmitoylphosphatidylcholine (DPPC), 1,2-distearoylphosphatidylethanolamine-methoxy-polyethyleneglycol (DSPE-PEG_{2000}-OMe), and 1,2-distearoyl-*sn*-glycero-3-phosphatidylethanolamine-polyethyleneglycol-maleimide (DSPE-PEG_{2000}-Mal) were purchased from NOF Corporation (Tokyo, Japan). Doxorubicin (Dox) was purchased from Sigma–Aldrich Co. (St. Louis, MO, USA). For cell culture, Dulbecco's Modified Eagle's Medium (DMEM) was purchased from Kohjin Bio Co. Ltd. (Tokyo, Japan). Endothelial Cell Growth Medium Kit was purchased from Cell Applications, Inc. (San Diego, CA, USA). Fetal bovine serum (FBS) was purchased from Equitech Bio Inc. (Kerrville, TX, USA). All other materials were used without further purification.

2.2. Preparation of liposomes and BLs

To prepare liposomes for BLs, DPPC and DSPE-PEG_{2000}-OMe were mixed at a molar ratio of 94:6. The liposomes were prepared by a reverse-phase evaporation method, as described previously [18–21]. In brief, all the reagents were dissolved in 1:1 (v/v) chloroform/diisopropylether. Phosphate-buffered saline was added to the lipid solution, and the mixture was sonicated and then evaporated at 47 °C. The organic solvent was completely removed, and the size of the liposomes was adjusted to less than 200 nm using extrusion equipment and a sizing filter (Nuclepore Track-Etch Membrane, 200 nm pore size, Whatman plc, UK). After being sized, the liposomes were passed through a sterile 0.45-μm syringe filter (Asahi Techno Glass Co., Chiba, Japan) for sterilization. For the fluorescent labeling of the lipid membrane, 1,1-dioctadecyl-3,3,3,3-tetramethyl-indocarbocyanine perchlorate (DiI: 0.1 or 1 mol% of total lipids) was added. The lipid concentration was measured using the Phospholipid C test (Wako Pure Chemical Industries, Ltd., Osaka, Japan). BLs were prepared from liposomes and perfluoropropane gas (Takachiho Chemical Inc., Co., Ltd., Tokyo, Japan). First, 5 mL sterilized vials containing 2 mL of liposome suspension (lipid concentration: 1 mg/mL) were filled with perfluoropropane gas, capped, and then pressurized with 7.5 mL of perfluoropropane gas. The vials were placed in a bath-type sonicator (42 kHz, 100 W, Bransonic 2510J-DTH, Branson Ultrasonics Co., Danbury, CT) for 5 min to form BLs. The mean size of the BLs was determined using light-scattering with a zeta potential/particle sizer (Nicomp 380ZLS, Santa Barbara, CA).

2.3. Preparation of AG73 peptide-modified liposomes and BLs

The Cys-AG73 peptide (CGG-RKRLQVQLSIRT) and a scrambled Cys-AG73T control peptide (CGG-LQQRRSVLRTKI) were synthesized manually using the 9-fluorenylmethoxycarbonyl (Fmoc)-based solid-phase strategy, prepared in the COOH terminal amide form, and purified by reverse-phase high-performance liquid chromatography. Liposomes composed of DPPC, DSPE-PEG_{2000}-OMe, and DSPE-PEG_{2000}-Mal at a molar ratio of 94:4:2 were prepared by a reverse-phase evaporation method. For the preparation of AG73 peptide-modified liposomes, adequate amounts of AG73 peptide were added to liposomes and gently mixed, as described previously [31,32]. In briefly, for coupling, AG73 peptide at a molar ratio of 5-fold DSPE-PEG_{2000}-Mal was added to the liposomes in the presence of tris(2-carboxyethyl)phosphine hydrochloride (TCEP: final concentration 20 mM), and the mixture was incubated for 6 h at room temperature to conjugate the cysteine of the Cys-AG73 peptide with the maleimide of the liposomes using a thioether bond. The resulting AG73 peptide-conjugated liposomes (AG73-liposomes) were dialyzed to remove any excess peptide. The AG73-liposomes were modified with 6 mol% PEG and 2 mol% peptides. AG73 peptide-modified BLs (AG73-BLs) were prepared from liposomes and perfluoropropane gas. The particle size of the liposomes and BLs was measured using a NICOMP 380ZLS. The measurement of particle sizing of the liposomes and BLs was repeated three times.

2.4. Cell lines and animals

Murine colorectal carcinoma cells (colon26) were cultured in DMEM that was supplemented with 10% FBS, penicillin (100 U/mL), and streptomycin (100 μg/mL) at 37 °C in a humidified 5% CO_2 atmosphere. Human umbilical vein endothelial cells (HUVEC) were purchased from Cell Applications, Inc. and cultured in Endothelial Cell Growth Medium Kit. All experiments were performed using HUVEC between passage 5 and 9.

Male BALB/c mice (6 weeks old) were purchased from Tokyo Laboratory Animals Science Co., Ltd. (Tokyo, Japan). All animal use and relevant experimental procedures were approved by the Tokyo University School of Pharmacy and Life Science Committee on the Care and Use of Laboratory Animals.

2.5. Flow cytometry and in vitro ultrasound imaging analysis

The specific attachment of BLs was determined by flow cytometry analysis [33,34]. A suspension of HUVEC (2×10^5 cells/mL) was mixed with DiI-labeled BLs (60 μg/sample) and incubated for 3 min at 4 °C. Subsequently, the cells were washed with phosphate-buffered saline (PBS), and the cell samples were examined by flow cytometry using an FACScan (Becton Dickinson, San Jose, CA, USA). The cell-associated DiI was excited with an argon laser (488 nm). Data were collected for 10,000 gated events and analyzed using the CELL Quest software program. The specific attachment and US imaging ability of BLs were determined by US imaging. HUVEC (3.7×10^5 cells/well) were seeded in a 6-well plate and incubated for 24 h at 37 °C in 5% CO_2. Then, BLs (300 μg/sample) were added to the plate. The plates were sealed with sterile tape and inverted for 5 min. The medium was removed, and subsequently, the cells were washed with DMEM containing 10% FBS. Then, B-mode recordings were made using a high-frequency ultrasound imaging system (NP60R-UBM, Nepa Gene, Co., Ltd., Chiba, Japan).

2.6. Perfusion chamber system assay

HUVEC (2×10^5 cells/well) were seeded in a cell culture insert (BD, NJ, USA) and incubated for 18 h at 37 °C in 5% CO_2. The cell culture insert was set at cell mixture culture system MK2000 (Yamato Scientific Co., Ltd., Japan.). Then, DiI-labeled BLs (5 μg/mL) were added, and refluxed for 5 min at 3.92 dyn/cm^2. The cells were washed with PBS twice and stained with Alexa Fluor 488-labeled phalloidin [2 units/well: Molecular Probes (Invitrogen, CA, USA.)]. Then, fluorescence images of the cells were analyzed using a BZ8100 (KEYENCE, Osaka, Japan).

2.7. Intratumoral localization of Bubble liposomes

Colon26 cells (1×10^6 cells/mouse) were inoculated subcutaneously in the right flank of mice. Ten days after tumor inoculation [when the tumor volume reached approximately 350 mm^3: the tumor volume was calculated using the following equation: tumor volume (mm^3) = longer diameter × (shorter one diameter)^2 × 0.5] ($n = 3$). DiI-labeled BLs were administered via the tail vein. The injected dose of lipid in each administration was 200 μg/mouse. At 20 min after injection of the BLs, the mice were sacrificed, and the tumors were dissected. These tissues were fixed in 10% paraformaldehyde substituted with 20% sucrose and were embedded in optimal cutting temperature compound (Sakura Finetech, Co. Ltd., Tokyo, Japan) and frozen at −80 °C. Tumor sections were prepared with a width of 20 μm and mounted on poly-L-lysine coated slides and fluorescently observed with a BZ-8100.

2.8. In vivo ultrasound imaging

For *in vivo* ultrasound (US) imaging, tumor-bearing mice (the tumor volume reached approximately 350 mm^3) were used ($n = 4$). The mice were anesthetized and their hair was removed using a depilatory cream. US imaging was performed with a dedicated small-animal high spatial-resolution imaging system (Vevo2100, VisualSonics). A 16 MHz linear transducer (GAIN: 25 dB, Frame Rate: 25 Hz, Dynamic Range: 50 dB) was fixed on a railing system. The dose of lipid injected in each experiment was 200 μg/mouse. For contrast-enhanced US imaging in the animals,

Table 1
Size of liposomes or Bubble liposomes.

	Mean diameter ± SD. (nm; $n = 3$)	
	Liposomes	Bubble liposomes
PEG-liposomes (non-labeled)	134.7 ± 52.1	600.8 ± 69.4
AG73-liposomes	153.2 ± 60.4	420.3 ± 54.9
AG73T-liposomes	143.5 ± 43.9	566.0 ± 75

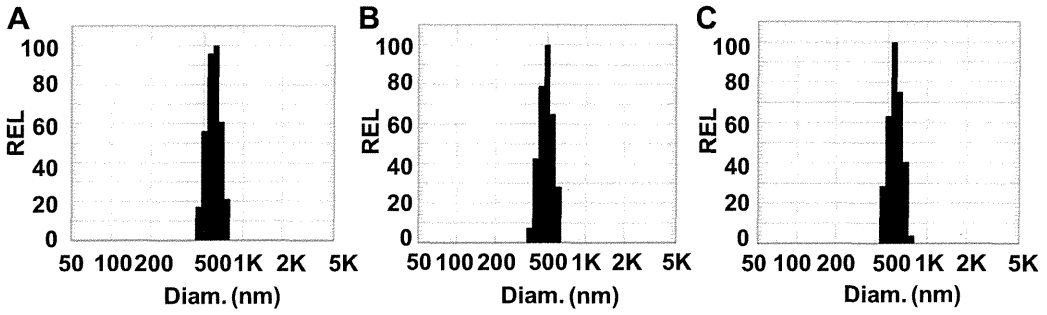

Fig. 1. Size distribution of Bubble liposomes (A) BLs (non-labeled), (B) AG73-BLs and (C) AG73T-BLs.

first we obtained US images before BLs administration as a reference. The different types of BLs were administered in a random order to minimize any bias. To facilitate clearance of BLs from the preceding imaging sessions, a 30 min delay was used between each imaging session. This delay between microbubble injection was chosen on the basis of previous findings [35,36]. Images representing the adherent BLs were displayed by the imaging system as green overlays on the contrast mode. In brief, the images were recorded digitally and analyzed offline by using commercially available high-resolution micro-US imaging software (Vevo2100, VisualSonics). The differences in image intensity determined by subtraction of the before and after administration images was automatically displayed by the software as a colored (green) overlay on the gray-scale images. In addition, image intensity was calculated by the software.

3. Results and discussion

3.1. Characteristics of AG73 peptide-modified liposomes and Bubble liposomes

First, we sought to prepare AG73 peptide-modified liposomes (AG73-L) and Bubble liposomes (AG73-BLs). As shown in Table 1, the mean particle diameter of the liposomes, including non-labeled and peptide-modified liposomes, ranged from 130 to 160 nm. The AG73 or AG73T peptide-modified liposomes did not aggregate [32]. The mean particle diameter of the BLs was larger and ranged from 400 to 600 nm, with a relatively narrow distribution (Fig. 1). The BLs could effectively entrap the imaging gas, which suggested that BLs could be used as a US contrast agent *in vitro* [15,16,20]. This result suggests that we could fabricate a nanosized lipid bubble.

3.2. Specific adhesion and in vitro US imaging ability of AG73 peptide-modified Bubble liposomes

To examine the specific adhesion of AG73-BLs to blood vessels, the fluorescence intensity of HUVEC was measured by flow cytometry analysis. As shown in Fig. 2(A), cell attachment of AG73-BLs to HUVEC was higher than that of non-labeled or AG73T peptide-modified BLs. The laminin-derived AG73 peptide is known as a ligand for syndecans, and it has been reported that syndecan-2 is highly expressed on HUVEC [29,30]. In addition, the AG73 peptide binds to the heparan sulfate side chains of syndecans [25]. Therefore, to study whether AG73-BLs can bind to syndecan-2 on the surface of HUVEC, the cells were treated with AG73-BLs and heparin [Fig. 2(B)]. Our data showed that cellular attachment of AG73-BLs was reduced by treatment with heparin. These results suggested that AG73-BLs could effectively target blood vessels via the syndecan-2 receptor. To elucidate the attachment and US imaging ability of AG73-BLs as an ultrasound agent, the ability of BLs was evaluated by US imaging after inverting the plate causing the ascending force of BLs [Fig. 3(A)]. As shown in Fig. 3(A), the cells treated with AG73-BLs could be imaged, whereas cells treated with non-labeled or AG73T peptide-modified BLs could not be detected. When we also calculated the US image intensity, the image intensity of AG73-BLs was ten times higher than other BLs [Fig. 3(B)]. These results suggest that AG73-BLs could be helpful as an ultrasound imaging agent for blood vessels.

3.3. Perfusion chamber analysis

Next, to determine whether AG73-BLs as a targeting ultrasound imaging agents could be used in a clinical setting, we investigated the attachment of AG73-BLs on HUVEC using a perfusion chamber system (Fig. 4). Perfusion chambers mimic circulatory blood flow *in vivo* [37–40]. Perfusion chamber experiments were performed to confirm binding of BLs to HUVEC under flow shear stress (flow rate of 3.92 dyn/cm^2, corresponding to high shear stress) [38]. As shown in Fig. 4(B–D), we could only observe DiI-labeled AG73-BLs attached

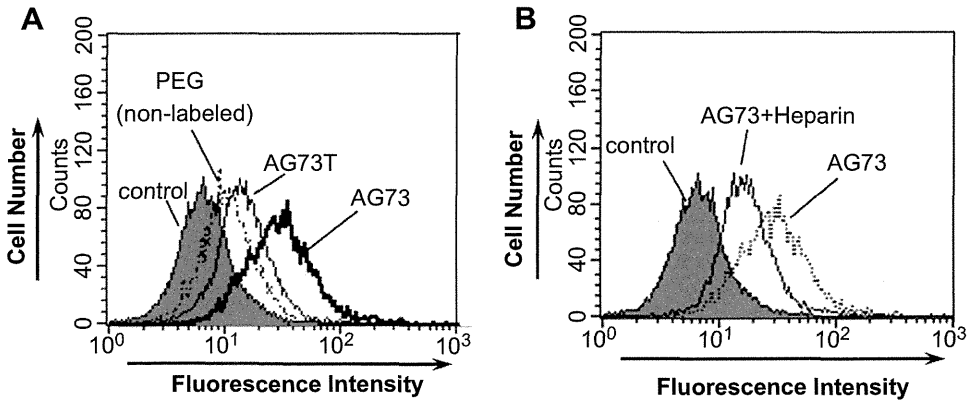

Fig. 2. Specific adhesion activity of AG73-modified Bubble liposomes to HUVEC. (A) HUVEC were treated with DiI-labeled BLs (PEG), AG73-BLs or AG73T-BLs for 3 min at 4 °C. The fluorescence intensity was measured by flow cytometry. (B) HUVEC was treated with DiI-labeled AG73-modified BL or AG73-modified BL + heparin in the same way.

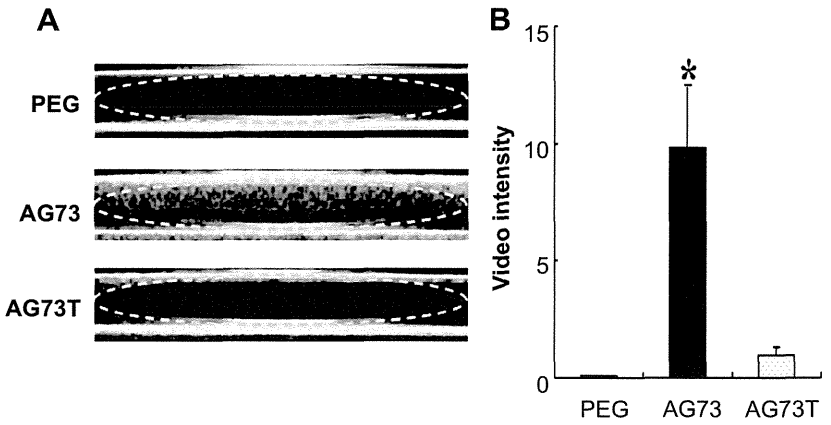

Fig. 3. Ultrasonographic images of AG73-modified Bubble liposomes on HUVEC (A). HUVEC were treated with non-labeled (PEG), AG73-BLs or AG73T-BLs for 5 min at room temperature. Then HUVEC were observed by US imaging (sample frequency: 80 kHz, pulse frequency: 18 MHz, Sweep: 20, B-mode). US image intensity (yellow circle) was calculated by NIH image (B). $^{*}P < 0.01$ compared with AG73T, PEG-Bubble liposomes. (For interpretation of the references to color in this figure legend, the reader is referred to the web version of this article.)

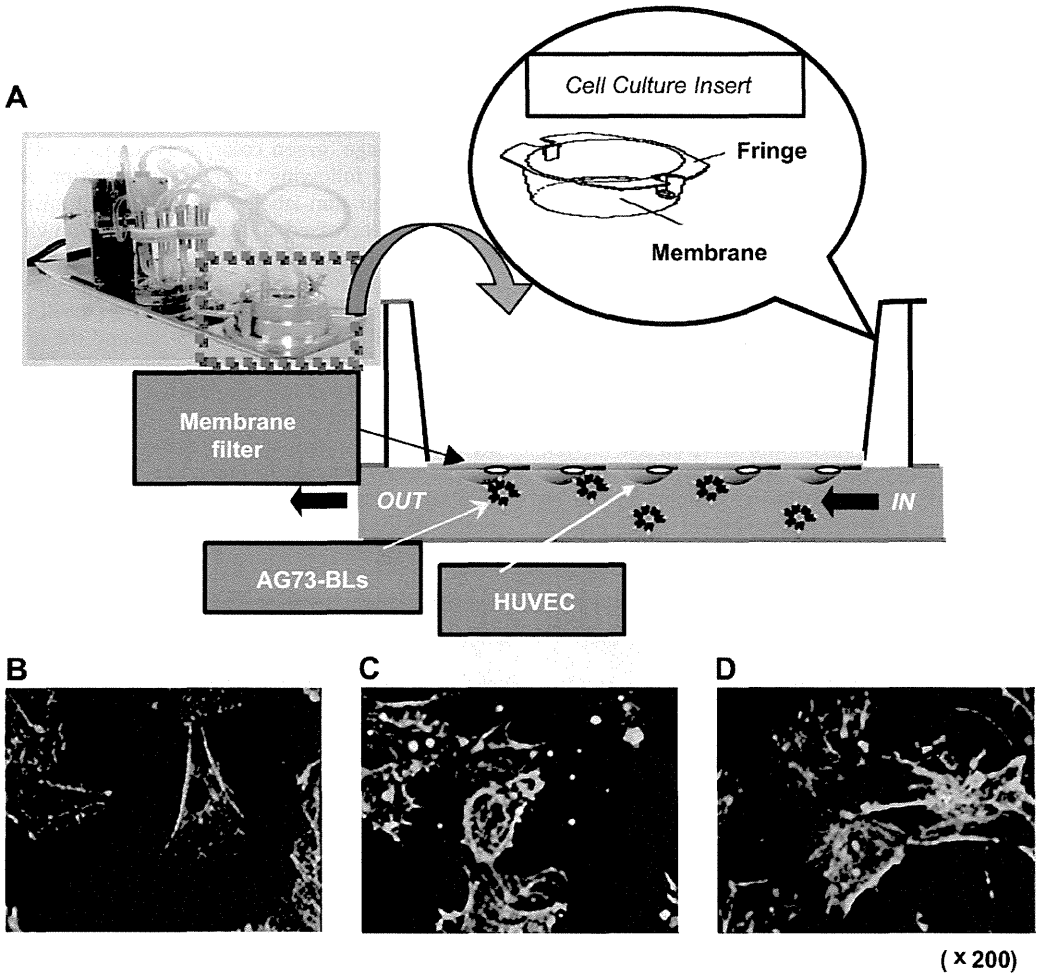

Fig. 4. Adhesion activity of AG73-modified Bubble liposomes in perfusion chamber system (A). HUVEC were treated with DiI-labeled BLs (B), AG73-BLs (C) or AG73T-BLs (D) for 5 min at room temperature in a perfusion chamber system. This system put shear stress (3.92 dyn/cm^2) on HUVEC. Subsequently, the cells were fixed and stained for α-actin. Actin was visualized with Alexa488-labeled phalloidin (green). The stained cells were examined using a fluorescence microscope.

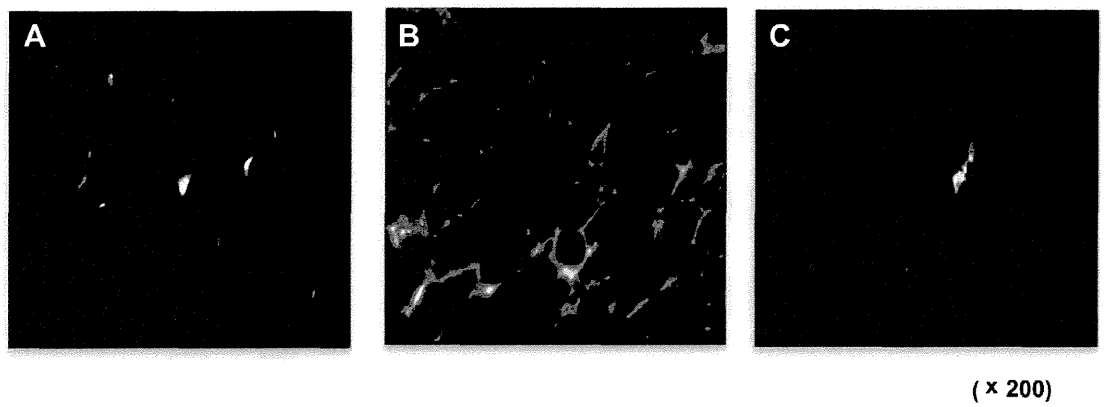

Fig. 5. Intratumoral distribution of AG73-modified Bubble liposomes. Colon26 bearing mice were intravenously injected with Dil-labeled BLs (A), AG73-BLs (B) or AG73T-BLs (C). At 20 min after injection, the tumors were removed, and then frozen-sections (20 μm) were prepared. Frozen-sections were examined by a fluorescence microscope.

to HUVEC. No cellular attachment of other BLs was observed. It have been reported that a fluid shear stress of 2 dyn/cm^2 corresponds to the stress of occurring in human arteries *in vivo* [37]. In this study, we carried out perfusion chamber experiments under the 3.92 dyn/cm^2. These results suggest that AG73-BLs could strongly associate with HUVEC and may be applied in clinical settings.

3.4. Intratumoral distribution of AG73-BLs

We have showed that AG73-BLs have a potential as a blood vessel targeting ultrasound imaging agent *in vitro*. To evaluate the targeting effect of AG73-BLs in tumor tissue, we examined the intratumoral localization of AG73-BLs. As shown in Fig. 5, the tumor sections treated with AG73-BLs showed high intensity and broad areas with red fluorescence, whereas tumor sections treated with non-labeled or AG73T peptide-modified BLs showed sparse red fluorescence. Since at 20 min after injection of the BLs, the tumor sections treated with non-labeled BLs have few red fluorescence, we conclude that BLs cannot accumulate in the tumor by an enhanced permeability retention (EPR) effect, which is phenomena that nanoparticles exhibit a prolonged systemic circulation time and increased tumor localization [41]. Therefore, this result suggests that the BLs retains the ultrasound imaging gas *in vivo* after administration. Previously, we also have reported that AG73 peptide-modified liposomes (AG73-L) were mainly bound to intratumoral vessels and were partially extravasated in the tumor. In addition, distribution of AG73-L to normal tissues (heart, liver, spleen, and kidney) differed little from that of PEG-liposomes [32]. This result suggests that AG73-BLs could target blood vessels in tumor tissue and be useful in *in vivo*.

3.5. In vivo US imaging

To evaluate the potential of the AG73-BLs as a blood vessel-targeting ultrasound contrast agent *in vivo*, we performed ultrasound imaging in tumor-bearing mice. No animals suffered any injuries, including burn, edema, and death, during this experiment. Contrast image (green color) was detected as an increased scattering signal following reference subtraction of the pre-injection image. When non-labeled BLs were administered, the contrast image was decreased at 1 min (data not shown). When AG73-BLs were administered, the contrast image was maintained at 4 min (Fig. 6). Moreover, Fig. 7 shows a time–intensity curve (TICs) generated after an intravenous injection for BLs. The shapes of the TICs were different for the AG73-BLs and the non-labeled BLs. The accumulation of AG73-BLs in the tumors and the difference between the TICs of the non-labeled BLs and the AG73-BLs could be explained by the circulation and attachment to the tumor vessels by AG73-BLs immediately after administration [Fig. 7(A)]. These results show that AG73-BLs could target tumor vessels whereas non-labeled BLs could not. In this study, we succeeded in developing an ultrasound imaging agent which targeted tumor vessels

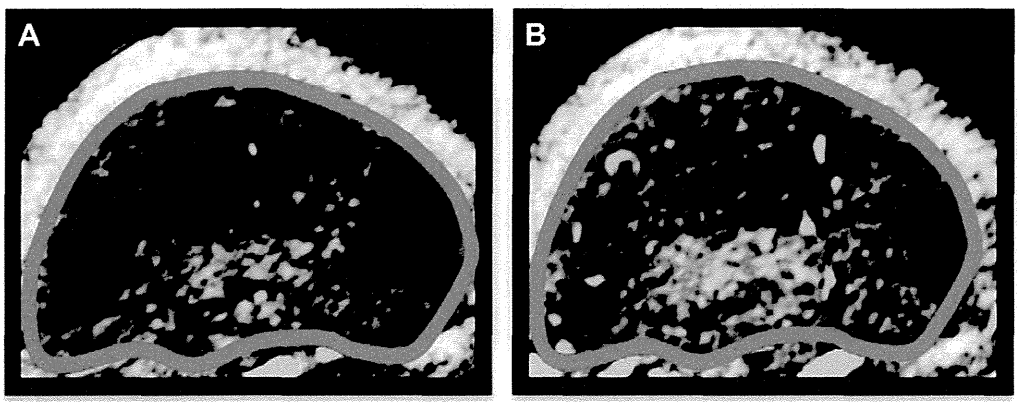

Fig. 6. Ultrasound imaging of AG73-modified Bubble liposomes. Colon26 bearing mice were intravenously injected with non-labeled (A), AG73-modified BLs (B). US images obtained 4 min after intravenous administration. The purple circles indicate the tumor.

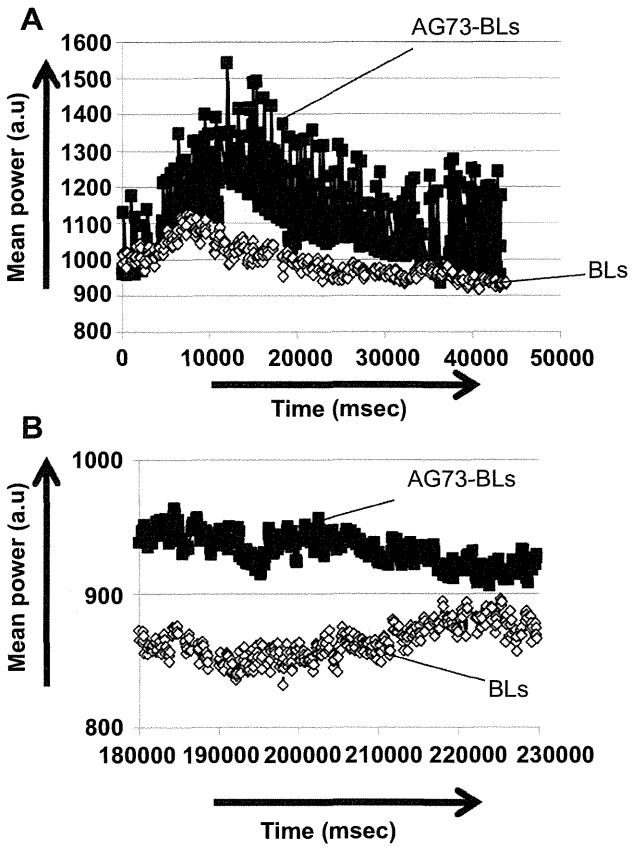

Fig. 7. Ultrasound imaging effect of AG73-modified Bubble liposomes on time–intensity curve. Colon26 bearing mice were intravenously injected with non-labeled and AG73-modified BLs. Time-intensity curves were obtained 0–1 min (A) and 3–4 min after intravenous administration (B).

and allowed imaging. However, in order for AG73-BLs to be an ideal ultrasound contrast agent in clinical practice, it is necessary to have a longer lasting image. Therefore, we think that there is a need to improve the AG73-BLs, such as modification of the peptide ratio and/or optimization of the lipid composition.

We have previously reported that Bubble liposomes can function as a gene and siRNA delivery tool by applying them with US exposure *in vitro* and *in vivo* [18–21]. Furthermore, we have succeeded to prepare BLs containing cationic lipids, which are expected to have widespread application as delivery tools for various molecules possessing negative electric charges (siRNA or pDNA etc.) for systemic delivery into a targeted organ or tissues [20,21]. Therefore, it might be expected that AG73-BLs containing drugs or genes may be a useful tool for tumor-selective drug or gene delivery systems in combination with US exposure and lead to beneficial clinical applications for cancer therapy.

4. Conclusion

In this study, AG73 peptide-modified Bubble liposomes (AG73-BLs) were developed to target blood vessels and to enhance the contrast as an ultrasound imaging agent. The AG73 peptide is a notably suitable targeting molecule because it is known to be a ligand for syndecans, which are expressed in neovascular vessels. The size of AG73-BLs was small (approximately 500 nm). The attachment of AG73-BLs was higher than that of control BLs (non-labeled BLs and AG73T-BLs). In addition, AG73-BLs bound intratumoral vessels within the tumor. Moreover, ultrasound imaging with AG73-BLs specifically imaged for intratumoral vessels and enhanced the contrast and image for a longer examination time than non-labeled BLs. Thus, AG73-BLs have the potential to become a useful ultrasound contrast agent in clinical field for diagnosis based on US imaging.

Acknowledgments

We are grateful to Prof. Katsuro Tachibana (Department of Anatomy, School of Medicine, Fukuoka University) for technical advice regarding the induction of cavitation with US and to Mr. Yasuhiko Hayakawa, and Mr. Kosho Suzuki (NEPA GENE CO., LTD.) for technical advice regarding exposure to US. This study was supported by an Industrial Technology Research Grant (04A05010) from the New Energy and Industrial Technology Development Organization (NEDO) of Japan and a Grant-in-aid for Exploratory Research (18650146) from the Japan Society for the Promotion of Science, a Grant-in-Aid for Scientific Research (B) (20300179) from the Japan Society for the Promotion of Science.

References

[1] Willmann J,K, van Bruggen N, Dinkelborg L,M, Gambhir S,S. Molecular imaging in drug development. Nat Rev Drug Discov 2008;7:591–607.
[2] Lindner J,R. Microbubbles in medical imaging: current applications and future directions. Nat Rev Drug Discov 2004;3:527–33.
[3] Wilson S,R, Burns P,N. Microbubble-enhanced US in body imaging: what role? Radiology 2010;257(1):24–39.
[4] Deshpande N, Needles A, Willmann J,K. Molecular ultrasound imaging: current status and future directions. Clin Radiol 2010;65(7):567–81.
[5] Danila M, Popescu A, Sirli R, Sporea I, Martie A, Sendroiu M. Contrast enhanced ultrasound (CEUS) in the evaluation of liver metastases. Med Ultrason 2010; 12(3):233–7.
[6] Kiessling F, Huppert J, Palmowski M. Functional and molecular ultrasound imaging: concepts and contrast agents. Curr Med Chem 2009;16:627–42.
[7] Klibanov A,L. Ligand-carrying gas-filled microbubbles: ultrasound contrast agents for targeted molecular imaging. Bioconjug Chem 2005;16:9–17.
[8] Dayton P,A, Rychak J,J. Molecular ultrasound imaging using microbubble contrast agents. Front Biosci 2007;12:5124–42.
[9] Ferrara K,W, Borden M,A, Zhang H. Lipid-shelled vehicles: engineering for ultrasound molecular imaging and drug delivery. Acc Chem Res 2009;42(7): 881–92.
[10] Allen T,M, Hansen C, Martin F, Redemann C, Yau-Young A. Liposomes containing synthetic lipid derivatives of poly(ethyleneglycol) show prolonged circulation half-lives in vivo. Biochim Biophys Acta 1991;1066:29–36.
[11] Blume G, Cevc G. Liposomes for the sustained drug release in vivo. Biochim Biophys Acta 1990;1029:91–7.
[12] Harata M, Soda Y, Tani K, Ooi J, Takizawa T, Chen M, et al. CD19-targeting liposomes containing imatinib efficiently kill Philadelphia chromosome-positive acute lymphoblastic leukemia cells. Blood 2004;104:1442–9.
[13] Maruyama K, Yuda T, Okamoto A, Kojima S, Suginaka A, Iwatsuru M. Prolonged circulation time in vivo of large unilamellar liposomes composed of distearoyl phosphatidylcholine and cholesterol containing amphipathic poly(ethylene glycol). Biochim Biophys Acta 1992;1128:44–9.
[14] Maruyama K, Ishida O, Kasaoka S, Takizawa T, Utoguchi N, Shinohara A, et al. Intracellular targeting of sodium mercaptoundecahydrododecaborate (BSH) to solid tumors by transferrin-PEG liposomes, for boron neutron-capture therapy (BNCT). J Control Release 2004;98:195–207.
[15] Suzuki R, Takizawa T, Negishi Y, Hagisawa K, Tanaka K, Sawamura K, et al. Gene delivery by combination of novel liposomal bubbles with perfluoropropane and ultrasound. J Control Release 2007;117:130–6.
[16] Suzuki R, Takizawa T, Negishi Y, Utoguchi N, Maruyama K. Effective gene delivery with novel liposomal bubbles and ultrasonic destruction technology. Int J Pharm 2008;354:49–55.
[17] Suzuki R, Takizawa T, Negishi Y, Utoguchi N, Sawamura K, Tanaka K, et al. Tumor specific ultrasound enhanced gene transfer in vivo with novel liposomal bubbles. J Control Release 2008;125:137–44.
[18] Negishi Y, Matsuo K, Endo-Takahashi Y, Suzuki K, Matsuki Y, Takagi N, et al. Delivery of an angiogenic gene into ischemic muscle by novel bubble liposomes followed by ultrasound exposure. Pharm Res 2011;28:712–9.
[19] Negishi Y, Tsunoda Y, Endo-Takahashi Y, Oda Y, Suzuki R, Maruyama K, et al. Local gene delivery system by bubble liposomes and ultrasound exposure into joint synovium. J Drug Deliv 2011;2011. 203986.
[20] Endo-Takahashi Y, Negishi Y, Kato Y, Suzuki R, Maruyama K, Aramaki Y. Efficient siRNA delivery using novel siRNA-loaded bubble liposomes and ultrasound. Int J Pharm 2012;422(1-2):504–9.

[21] Negishi Y, Endo-Takahashi Y, Matsuki Y, Kato Y, Takagi N, Suzuki R, et al. Systemic delivery systems of angiogenic gene by novel bubble liposomes containing cationic lipid and ultrasound exposure. Mol Pharm 2012;9(6): 1834–40.
[22] Kerbel R, Folkman J. Clinical translation of angiogenesis inhibitors. Nat Rev Cancer 2002;2:727–39.
[23] Cross M,J, Claesson-Welsh L. FGF and VEGF function in angiogenesis: signalling pathways, biological responses and therapeutic inhibition. Trends Pharmacol Sci 2001;22:201–7.
[24] Carey D,J. Syndecans: multifunctional cell-surface co-receptors. Biochem J 1997;327:1–16.
[25] Hoffman M,P, Nomizu M, Roque E, Lee S, Jung DW, Yamada Y, et al. Laminin-1 and laminin-2 G-domain synthetic peptides bind syndecan-1 and are involved in acinar formation of a human submandibular gland cell line. J Biol Chem 1998;273:28633–41.
[26] Suzuki N, Ichikawa N, Kasai S, Yamada M, Nishi N, Morioka H, et al. Syndecan binding sites in the laminin alpha1chain G domain. Biochemistry 2003;42: 12625–33.
[27] Couchman J,R. Syndecans: proteoglycan regulators of cell-surface microdomains? Nat Rev Mol Cell Biol 2003;4:926–37.
[28] Fears C,Y, Gladson C,L, Woods A. Syndecan-2 is expressed in the microvasculature of gliomas and regulates angiogenic processes in microvascular endothelial cells. J Biol Chem 2006;281:14533–6.
[29] Halden Y, Rek A, Atzenhofer W, Szilak L, Wabnig A, Kungl A,J. Interleukin-8 binds to syndecan-2 on human endothelial cells. Biochem J 2004;377(Pt 2): 533–8.
[30] Mertens G, Cassiman JJ, Van den Berghe H, Vermylen J, David G. Cell surface heparan sulfate proteoglycans from human vascular endothelial cells. Core protein characterization and antithrombin III binding properties. J Biol Chem 1992;267:20435–43.
[31] Negishi Y, Omata D, Iijima H, Takabayashi Y, Suzuki K, Endo Y, et al. Enhanced laminin-derived peptide AG73-mediated liposomal gene transfer by bubble liposomes and ultrasound. Mol Pharm 2010;7(1):217–26.
[32] Negishi Y, Hamano N, Omata D, Fujisawa A, Manandhar M, Nomizu M, et al. Effect of doxorubicin-encapsulating AG73 peptide-modified liposomes on tumor selectively and cytotoxicity. Results Pharm Sci 2011;1: 68–75.
[33] Hwang T, Han HD, Song CK, Seong H, Kim JH, Chen X, et al. Anticancer drug-phospholipid conjugate for enhancement of intracellular drug delivery. Macromol Symp 2007;249–250:109–15.
[34] Mannell H, Pircher J, Räthel T, Schilberg K, Zimmermann K, Pfeifer A, et al. Targeted endothelial gene delivery by ultrasonic destruction of magnetic microbubbles carrying lentiviral vectors. Pharm Res 2012;5:1282–94.
[35] Weller G,E, Wong M,K, Modzelewski R,A, Lu E, Klibanov A,L, Wagner W,R, et al. Ultrasonic imaging of tumor angiogenesis using contrast microbubbles targeted via the tumor-binding peptide arginine-arginine-leucine. Cancer Res 15 Jan 2005;65(2):533–9.
[36] Willmann J,K, Paulmurugan R, Chen K, Gheysens O, Rodriguez-Porcel M, Lutz A,M, et al. US imaging of tumor angiogenesis with microbubbles targeted to vascular endothelial growth factor receptor type 2 in mice. Radiology 2008; 246(2):508–18.
[37] Franke R,P, Gräfe M, Schnittler H, Seiffge D, Mittermayer C, Drenckhahn D. Induction of human vascular endothelial stress fibres by fluid shear stress. Nature 1984;307(5952):648–9.
[38] Giavazzi R, Foppolo M, Dossi R, Remuzzi A. Rolling and adhesion of human tumor cells on vascular endothelium under physiological flow conditions. J Clin Invest 1993;92(6):3038–44.
[39] Yamawaki H, Lehoux S, Berk B,C. Chronic physiological shear stress inhibits tumor necrosis factor-induced proinflammatory responses in rabbit aorta perfused ex vivo. Circulation 2003;108(13):1619–25.
[40] Pysz M,A, Foygel K, Rosenberg J, Gambhir S,S, Schneider M, Willmann J,K. Antiangiogenic cancer therapy: monitoring with molecular US and a clinically translatable contrast agent (BR55). Radiology 2010;256(2):519–27.
[41] Maeda H, Wu J, Sawa T, Matsumura Y, Hori K. Tumor vascular permeability and the EPR effect in macromolecular therapeutics: a review. J Control Release 2000;65:271–84.

European Journal of Pharmaceutical Sciences xxx (2013) xxx–xxx

Contents lists available at ScienceDirect

European Journal of Pharmaceutical Sciences

journal homepage: www.elsevier.com/locate/ejps

Tissue distribution and safety evaluation of a claudin-targeting molecule, the C-terminal fragment of *Clostridium perfringens* enterotoxin

Xiangru Li, Rie Saeki, Akihiro Watari, Kiyohito Yagi, Masuo Kondoh *

Laboratory of Bio-Functional Molecular Chemistry, Graduate School of Pharmaceutical Sciences, Osaka University, Suita, Osaka 565-0871, Japan

ARTICLE INFO

Article history:
Received 2 April 2013
Received in revised form 25 October 2013
Accepted 25 October 2013
Available online xxxx

Keywords:
Claudin
Clostridium perfringens enterotoxin
Kidney
Liver
Tissue distribution

ABSTRACT

We previously found that claudin (CL) is a potent target for cancer therapy using a CL-3 and -4-targeting molecule, namely the C-terminal fragment of *Clostridium perfringens* enterotoxin (C-CPE). Although CL-3 and -4 are expressed in various normal tissues, the safety of this CL-targeting strategy has never been investigated. Here, we evaluated the tissue distribution of C-CPE in mice. Ten minutes after intravenous injection into mice, C-CPE was distributed to the liver and kidney (24.0% and 9.5% of the injected dose, respectively). The hepatic level gradually fell to 3.2% of the injected dose by 3 h post-injection, whereas the renal C-CPE level gradually rose to 46.5% of the injected dose by 6 h post-injection and then decreased. A C-CPE mutant protein lacking the ability to bind CL accumulated in the liver to a much lesser extent (2.0% of the dose at 10 min post-injection) than did C-CPE, but its renal profile was similar to that of C-CPE. To investigate the acute toxicity of CL-targeted toxin, we intravenously administered C-CPE-fused protein synthesis inhibitory factor to mice. The CL-targeted toxin dose-dependently increased the levels of serum biomarkers of liver injury, but not of kidney injury. Histological examination confirmed that injection of CL-targeted toxin injured the liver but not the kidney. These results indicate that potential adverse hepatic effects should be considered in C-CPE-based cancer therapy.

1. Introduction

Most lethal cancers are derived from epithelial tissues (Jemal et al., 2008), and many therapeutic strategies targeting such cancers have been developed. Selective delivery of anti-cancer agents to cancer cells is a popular anti-cancer strategy (Adair et al., 2012; Yewale et al., 2013). Many membrane proteins that are present at much higher levels in cancer cells than in normal cells have been identified. Antibodies have recently become available as anti-cancer drugs targeting breast cancer (pertuzumab, directed against human epidermal growth factor receptor-2) and colon cancer (panitumumab, directed against epidermal growth factor receptor) (Dent et al., 2013; Zouhairi et al., 2011).

Normal epithelial cells develop complex intercellular tight junctions (TJs) that prevent the free movement of solutes across epithelial cell sheets and of membrane proteins and lipids between apical and basolateral membranes (Furuse and Tsukita, 2006; Rodriguez-Boulan and Nelson, 1989; Vermeer et al., 2003). In contrast, TJ functionality is frequently abnormal in transformed epithelial cells. As a result, cellular polarity and intercellular contact are often lost, both in the early stages of carcinogenesis and in advanced tumors (Wodarz and Nathke, 2007). Such findings indicate that the membrane proteins of TJs, which are difficult to access in normal epithelia but are exposed in malignant cells, may be candidate targets for cancer therapy.

Freeze-fracture replica electron microscopy has shown that TJs present as a series of continuous, anastomotic, intramembranous particulate strands, or fibrils (Farquhar and Palade, 1963; Staehelin, 1973). The TJ-containing strands are composed of both intracellular and integral membrane proteins, including claudin (CL) (Anderson and Van Itallie, 2009). CL comprises a tetraspan protein family with 27 members (Mineta et al., 2011). Interestingly, the expression of CL-3 or -4, or both, is increased in breast, gastric, intestinal, ovarian, pancreatic, and prostatic carcinomas (Singh et al., 2010; Tsukita et al., 2008; Turksen and Troy, 2011).

Clostridium perfringens enterotoxin (CPE) causes food poisoning in humans (McClane and Chakrabarti, 2004). CL-3 and CL-4 serve as receptors for CPE, and CPE is cytotoxic to cells expressing these CLs (Long et al., 2001; Sonoda et al., 1999). Intratumoral administration of CPE attenuates pancreatic tumor growth, and intraperitoneal administration of CPE inhibits ovarian tumor growth

Abbreviations: ALT, alanine aminotransferase; AST, aspartate aminotransferase; BSA, bovine serum albumin; BUN, blood urea nitrogen; CL, claudin; CPE, *Clostridium perfringens* enterotoxin; C-CPE, C-terminal fragment of CPE; FACS, fluorescence-activated cell sorter; PBS, phosphate-buffered saline; PSIF, protein synthesis inhibitory factor; TJ, tight junction.

* Corresponding author. Tel.: +81 6 6879 8196; fax: +81 6 6879 8199.
E-mail address: masuo@phs.osaka-u.ac.jp (M. Kondoh).

0928-0987/$ - see front matter © 2013 Published by Elsevier B.V.
http://dx.doi.org/10.1016/j.ejps.2013.10.018